ELECTRON MICROSCOPE LOCALIZATION OF ACETYLCHOLINESTERASE AND BUTYRYLCHOLINESTERASE IN THE SUPERIOR CERVICAL GANGLION OF THE CAT

I. Normal Ganglion

RICHARD DAVIS and GEORGE B. KOELLE

From the Department of Pharmacology, School of Medicine/G3, University of Pennsylvania, Philadelphia, Pennsylvania 19104

ABSTRACT

The distributions of acetylcholinesterase (AChE) and butyrylcholinesterase (BuChE) in the superior cervical ganglion (SCG) of the cat were determined by electron microscopy (EM) with the bis-(thioacetoxy)aurate (I), or $Au(TA)_2$, method. Before the infusion of fixative, one of the enzymes was selectively, irreversibly inactivated in vivo, as confirmed by light microscope (LM) examination of sections of the stellate ganglion stained by the more specific copper thiocholine method. Physostigmine-treated controls, for inhibition of AChE or BuChE, were stained concomitantly with tissue for enzyme localization by the $Au(TA)_2$ method for EM examination in each experiment. It was concluded that most of the AChE of the cat SCG is present in the plasma membranes of the preganglionic axons and their terminals, and in the dendritic and perikaryonal plasma membranes of the postsynaptic ganglion cells. BuChE is confined largely to the postsynaptic neuronal plasma membranes. Reasons for the discrepancies between the localizations found by the present direct EM observations and those deduced earlier from LM comparisons of normal and denervated SCG are discussed. It is proposed that a trophic factor released by the preganglionic terminals is probably required for the synthesis of postsynaptic neuronal AChE, and that BuChE may serve as a precursor of AChE at that site.

KEY WORDS acetylcholinesterase · butyrylcholinesterase · cholinesterases · electron microscopy · ganglia · histochemistry · superior cervical ganglion · sympathetic nervous system

Early light microscope (LM) histochemical comparisons of the distributions of acetylcholinesterase (acetylcholine hydrolase, EC 3.1.1.7, AChE) and butyrylcholinesterase (acylcholine acyl-hydrolase, pseudocholinesterase, EC 3.1.1.8, BuChE) in the normal and preganglionically denervated superior cervical ganglion (SCG) of the cat, by the highly specific copper thiocholine (CuThCh) method, led to certain deductions regarding the cytological localization of the two enzymes beyond the limits of resolution afforded by LM (29, 31, 42). In the normal ganglion, staining for both

enzymes was observed throughout the neuropil, and intense staining for AChE was noted also in the perikarya of occasional (<1%, see reference 23) cholinergic ganglion cells. Within a few days after preganglionic denervation, there was a nearly total disappearance of AChE-staining from the neuropil but only a relatively small decrease in the intensity of staining for BuChE. This pattern remained essentially unchanged for several weeks, and was consistent with the results of quantitative studies (35, 62). From this and other evidence it was concluded that, in the normal ganglion, AChE is confined largely to the preganglionic fibers and their terminals, and BuChE to the capsular glial or Schwann cells.

A decade ago it was possible with the gold-thiolacetic acid (37) and gold-thiocholine (38) methods to demonstrate by electron microscopy (EM) the discrete localization of AChE and pseudo-ChE at the pre- and postjunctional membranes of the mouse motor endplate, with a minimum of end product in the junctional cleft (10). However, neither of these methods provided satisfactory EM localization of the enzymes in the SCG, where the synaptic clefts and other intermembranous distances are considerably narrower, and AChE is present at lower concentration and in a more soluble, possibly different isoenzymatic form (41). These obstacles have since been largely overcome. The bis-(thioacetoxy) aurate (I), or $Au(TA)_2$, method, in which both the substrate and capturing agent are present in a readily penetrating single complex, $(Au[TA]_2)^-$, permits extremely precise localization of the immediately formed final reaction product, aurous sulfide; artifacts due to diffusion or translocation of the finely granular, electron-opaque precipitate from sites of enzyme activity are thus minimized (33, 36). In addition, procedures have been developed for the selective, irreversible inactivation of either AChE or BuChE in vivo (34, 43), and conditions of prefixation with buffered formaldehyde have been established that afford an acceptable compromise between degree of inactivation of the enzymes and limitation of their diffusion with a reasonable degree of morphological preservation (35).

The conclusions from the present, direct EM observations of the cytological localizations of AChE and BuChE in the cat SCG are at considerable variance with those of the earlier LM studies, which were based largely on the aforementioned indirect evidence. The most likely reasons for the discrepancies and their implications are considered in the Discussion.

MATERIALS AND METHODS

Denervation

In all EM investigations, the right, normal SCG was compared with the left SCG which had been denervated preganglionically 6–35 days previously. Findings in the denervated ganglia will be described in a subsequent paper. Cats were anesthetized with sodium pentobarbital, 35 mg/kg, intraperitoneally, and under semisterile conditions the contents of the left carotid sheath were exposed just caudad to the larynx; the common carotid artery was separated and a 1.5–2-cm segment of the remainder (vagosympathetic trunk and internal jugular vein) was excised between silk ligatures. After the skin incision was sutured, the cat was given an intramuscular injection of 1.0 ml of Combiotic (procaine penicillin G plus dihydrostreptomycin sulfate, Pfizer Chemicals Div., Pfizer, Inc., New York).

Selective Inactivation of BuChE or AChE

The cat was anesthetized as before, and either BuChE or AChE was irreversibly, selectively inactivated by minor modifications of procedures described previously (34, 43). BuChE was inactivated by the intravenous injection of 3.0 μmol of tetramonoisopropyl pyrophosphortetramide (iso-OMPA)/kg, which causes inactivation of over 98% of the ganglionic BuChE with no detectable loss of AChE. For the selective inactivation of AChE, the femoral artery was first catheterized to record blood pressure by means of a transducer coupled with a Physiograph, type DMP-4A (Narco-Bio-Systems, Inc., Houston, Texas), and the femoral vein was catheterized for injections; artificial respiration was administered by means of a tracheal catheter attached to a Palmer pump. After the injection of atropine sulfate (1.0 mg/kg, intraperitoneally, and 1.0 mg/kg, intravenously) and 3.0 mg mephentermine sulfate/kg, intravenously, to insure a patent airway and elevate the blood pressure, respectively, an intravenous infusion of the reversible, selective BuChE-inhibitor, 10-(α-diethylaminopropionyl) phenothiazine HCl (Astra 1397), was given in a total dose of 100–200 μmol/kg over approx. 15 min, as rapidly as possible without causing a lethal fall in blood pressure; after an interval of 3 min, this was followed by the intravenous injection of 2.0 μmol/kg of the irreversible inactivator of AChE and BuChE, isopropyl methylphosphonofluoridate (sarin). With this procedure, approx. 98% of the ganglionic AChE is inactivated irreversibly while approx. 50% of the BuChE is preserved (43). In the earlier experiments of this series, 2-diethoxyphosphinylthioethyldimethylamine acid oxalate (217 AO), 1.0 μmol/kg, was given in place of sarin

(34); however, under these conditions the latter compound produced a more favorable ratio of AChE/BuChE inactivation, and the inactivation is essentially irreversible.

Fixation

Approx. 15 min after the administration of the organophosphate anticholinesterase agent, the abdominal aorta was ligated just below the diaphragm; the chest was opened, the superior vena cava was incised, and 100 ml of chilled (8–10°C) 4% formaldehyde (prepared freshly from trioxymethylene) in Krebs-Ringer-calcium solution (18) were injected as rapidly as possible into the left ventricle via an 18-gauge needle. The normal and denervated SCGs were then removed, bisected longitudinally, and placed in the same fixative solution at approx. 2°C, along with the stellate and ciliary ganglia and carotid bodies, studies of which will be reported subsequently. One-half or both halves of each SCG were cut with a razor blade into chunks of approx. 1 mm^3. In some experiments, one-half was embedded in 7% agar and sectioned at 150 μm with a Smith-Farquhar Sorvall TC-2 tissue sectioner (DuPont Co., Instrument Products Div., Wilmington, Del.). However, after it was found that all reagents in the incubation medium apparently penetrate to a considerable depth in formalin-fixed tissue, only chunks were employed. The chunks and sections were left in the fixative at 2°C, with constant shaking at 120 cycles/min on a Fisher Rotator (Fisher Scientific Co., Pittsburgh, Pa.), for a total of 6 h from the time of perfusion with fixative *in situ*. They were then transferred to cold (2°C) Krebs-Ringer-calcium solution in which they were kept overnight. This type of fixation produces inactivation of approx. half the remaining AChE and BuChE activities of the ganglia (35), but appears to restrict effectively enzymatic diffusion (18) and produce acceptable anatomical preservation, as described below.

Copper Thiocholine Controls

In order to insure that the foregoing treatments in vivo produced essentially total inactivation of ganglionic BuChE or AChE, with preservation of most of the activity of the other enzyme, 10-μm cryostat sections were cut from a portion of the stellate ganglion that had been removed from each cat and fixed, and sections were placed on slides and stained by the more specific CuThCh method (31, 35) for examination by LM. The distributions of AChE and BuChE in this ganglion are qualitatively identical with those in the SCG (31), and its use here permitted all portions of the SCG to be processed for the EM studies. Slides were incubated for 30, 60, and 120 min in the standard media containing acetylthiocholine (AThCh) or butyrylthiocholine (BuThCh) as substrate. In addition, slides exposed previously to iso-OMPA, 10^{-3} M at 5°C for 1 h, were included; this produces essentially total inactivation of BuChE without detectable loss of AChE (34). Staining with AThCh but not with BuThCh, with or without iso-OMPA-treatment, was considered confirmation of selective inactivation of BuChE and preservation of AChE. Staining with BuThCh and lighter staining with AThCh, both of which were blocked by prior treatment with iso-OMPA, was accepted as evidence of AChE-inactivation and retention of BuChE. In all EM observations described below, these criteria of specificity were met.

Physostigmine Controls

Since the $Au(TA)_2$ method is not highly specific, it is necessary also to employ controls in which the enzyme being studied by EM is inhibited selectively in order to rule out staining due to enzymes other than AChE or BuChE, or to adsorption of the $(Au[TA]_2)^-$ complex or its breakdown products. For this purpose physostigmine, a highly selective inhibitor of AChE and BuChE, was employed. Only at sites where staining was blocked in corresponding physostigmine-treated tissues could AChE or BuChE activity be identified with certainty. Control chunks and Smith-Farquhar sections were kept in Krebs-Ringer-calcium solution containing 10^{-3} M physostigmine overnight to insure its adequate penetration; in the preincubation and incubation solutions, the concentration was reduced to 3×10^{-5} M.

Histochemical Reaction

The day after removal and fixation of tissue, chunks and sections were stained for AChE or BuChE by the $Au(TA)_2$ method described previously (36). During 1 h in the preincubation solution, 3–6 h in the incubation solution (changed hourly), and 1 h in the postincubation solution, the temperature was maintained at 5 ± 1°C and the vessels were shaken at 120 cycles/min on a Fisher Rotator. (All findings reported here were obtained with 6-h incubation.) The tissues were then transferred to the rinse solution (4% formaldehyde in maleate buffer, pH 7.0) and stored overnight at 4°C in order to insure adequate removal of the unreacted gold complex. Subsequently, they were postfixed in 1% OsO_4 in veronal acetate buffer (56) for 2 h at 4°C, dehydrated in a series of increasingly concentrated solutions of ethanol, and finally embedded in Epon 812 (50). Thin sections exhibiting yellow-to-gold interference colors were cut with a diamond knife on a Sorvall Porter-Blum MT-2 ultramicrotome (Du Pont Co., Instrument Products Div., Wilmington, Del.) and mounted on unfilmed copper grids; no further treatment to enhance contrast was employed. Yellow-to-gold sections were selected over thinner (silver) ones because the latter proved to be very fragile in the electron beam when not supported by a carbon film; also, the background intracellular detail such as unstained membranous elements, cytoplasm, and nucleoplasm appear in better contrast in the final

electron micrographs when moderately thicker sections are used. Sections were examined and micrographs were taken with a Philips EM-300 electron microscope, operated at 60 kV.

Many preliminary experiments were performed in the course of developing the foregoing procedures. For the final series, conducted as described above, nine normal (plus nine denervated) SCGs were examined for the localization of AChE, and six normal (plus five denervated) SCGs for BuChE.

RESULTS

Prelude

Cat SCG cells are multipolar (60), 25–32 μm in diameter (11), and >99% are probably adrenergic (23). Early LM cytological studies (3, 11, 60) described myelinated presynaptic axons from upper thoracic rami entering the ganglion via the cervical sympathetic trunk, losing their myelin, and branching extensively to synapse with one or several of the numerous (up to 10 or 12), long, extensively branched postsynaptic dendrites. No presynaptic axons were found to pass through the ganglion without synapsing (60). Axons of the ganglion cells were more difficult to identify, but those that could be traced did not appear to arise from the cell body, except in rare instances, but rather issued in nearly all cases from a dendrite, usually at some distance from the cell body (11). Furthermore, they did not appear to give off collateral branches, leading to the conclusion that postganglionic axons always end in the periphery and never in the ganglion of their origin (11, 60). On the basis of combined histological and physiological studies, it was concluded that a considerable number of the postganglionic axons acquire myelin sheaths before exiting via a postganglionic branch, and that the cervical sympathetic trunk and SCG contain few if any afferent fibers (3, 60). It should also be noted that small intensely fluorescent (SIF) or chromaffin cells, which are numerous in the rat SCG (17) and have been considered to function there as interneurons, are extremely rare in the cat SCG and consist almost exclusively of the type (II) devoid of efferent processes (69). Since EM studies of the cat SCG after preganglionic denervation failed to reveal the presence of any typical synaptic junctions (21, 45), it is unlikely that the normal ganglion contains significant numbers of interneurons or recurrent collaterals. The foregoing studies therefore are for the most part consistent with a simplified view of the cat SCG as a fairly uniform population of adrenergic cell bodies innervated by cholinergic preganglionic fibers; evidence for the presence of recurrent axon collaterals, interneurons, or afferent fibers is generally lacking.

Several EM studies (4, 14, 15, 21, 45, 57, 58) and reviews (20, 52) have dealt with the morphology of the cat SCG. For interpretation of the present findings, we are particularly indebted to the painstaking studies by Elfvin (14, 15) made on three-dimensional reconstructions from extensive numbers of serial sections. Elfvin described presynaptic unmyelinated axons of small diameter (0.1–0.3 μm) paralleling and winding around postsynaptic dendritic branches for considerable distances; at the repeated sites of axodendritic synaptic contract, the former widen into varicosities containing mitochondria and clusters of synaptic vesicles, and the postsynaptic membranes are usually thickened. The overwhelming majority of synaptic contacts found were axodendritic, occurring in reasonably close proximity to the perikarya, although rare axosomatic synapses were also present. Occasionally, two presynaptic axon profiles were found in close mutual contact without any Schwann cell cytoplasm intervening between their contiguous plasma membranes (15). Of much more frequent occurrence, however, were dendrodendritic contacts (14); one type consisted of a simple close association of plasma membranes, but a second, more complex type, sometimes with a length of 80–200 nm, was characterized by additional faintly opaque material on the cytoplasmic sides of the associated membranes. This latter type appeared structurally highly organized and might serve the function of adhesion (20), whereas any of the above contacts might be sites of metabolic interaction (14, 15). It was not determined whether any of these contacts are between neurites of a single or of separate neurons. Since essentially all of the processes issuing from the perikaryon must be dendrites, based on deCastro's descriptions cited above (11), Elfvin (14, 15) concentrated his study on these processes arising from the cell body, and the small presumably presynaptic axonal varicosities and terminals impinging upon them. The identification of these latter elements (or profiles) as presynaptic has since been confirmed by their disappearance after preganglionic denervation (21, 45). Unfortunately, Elfvin was not able to identify and

describe axons of the postsynaptic cells, even using serial sections. These processes had been described in LM silver-impregnated preparations by their length and lack of collateral branching (11), but they probably do not possess any fine structural features to distinguish them from the dendrites from which they originate. Schwann cells ensheathed or encapsulated almost all axons, dendrites, and cell bodies.

Our purpose in the present study was to elucidate as precisely as possible the location of both AChE and BuChE in or on the various cellular elements of the cat SCG, while using information gleaned from Elfvin's studies to identify correctly the profiles as portions of presynaptic axon, postsynaptic dendrite, cell body, or satellite cell.

The outermost 10–15 μm of a tissue chunk was usually less than optimally preserved, and it stained coarsely. Immediately beneath this layer was generally a region extending inward for at least 200–300 μm that was fairly well preserved and stained more or less consistently; our study was concentrated around the numerous dendritic branches and other structures in this portion. The core of the tissue chunk, 200–300 μm in diameter, was considered to be less reliably stained and was therefore avoided.

AChE Staining: Cats Treated with iso-OMPA in vivo for Selective Inactivation of BuChE

Myelinated axons are numerous throughout the ganglion, and nearly all exhibit intensely stained axolemmas (Figs. 1 and 2); as noted below, staining here and in all more distal regions of the axolemma was blocked by physostigmine. The aurous sulfide endproduct is seen as a finely granular deposit at intermediate or high magnification, and, even though the axolemma is heavily stained, the deposit does not appear to extend more than slightly into the intercellular space between it and the first layer of myelin (Fig. 1). The deposit is distributed over the entire axolemma, and is not arranged in a patchy or discontinuous manner. Myelin membranes are unstained as is the plasmalemma of the Schwann cell surrounding them. An occasional myelinated axon is present that is devoid of staining at the axolemma (Fig. 2); this is probably not due to inadequate penetration of reagents through the thick myelin covering since intra-axoplasmic structures such as mitochrondria and smooth endoplasmic reticulum (ER) membranes exhibit physostigmine-resistant (*vide infra*) staining of variable intensity. On the basis of the reports cited above, it is likely that these AChE-negative myelinated fibers are postsynaptic adrenergic axons, or possibly primary afferent fibers whose cells of origin lie craniad to the SCG. No staining is detectable at the neurofilaments or microtubules here or in the subsequent micrographs.

Unmyelinated axons can be identified positively as preganglionic only where they are near-terminal or comprise a varicosity possessing numerous 40–60 nm synaptic vesicles. In favorable profiles of these (Figs. 3 and 4), the axolemma appears to be completely and discretely stained, usually without the deposit extending into the adjacent intercellular space or appearing on apposed Schwann cell membranes. Within the axoplasm, staining is noted at vesicular structures and at mitochondrial membranes; however, the only stained structures that were rendered totally blank by physostigmine are occasional synaptic vesicles (Figs. 4–6). If lightly stained, the deposit appears to outline the vesicle membrane (Fig. 4); in other instances, it tends to fill the vesicle interior as well (Figs. 5 and 6). Adjacent Schwann cell plasma membranes are unstained, but the ER is stained (Figs. 3–6).

At axodendritic synapses the entireties of the plasma membranes of both axon and dendrite are stained, perhaps slightly more heavily at the site of junctional contact than in their adjacent continuations (Figs. 5 and 6). The synaptic clefts as well as other intercellular spaces are essentially devoid of deposit. The relative intensities of staining of the junctional membranes vary; these membranes are sometimes about equally stained as in Fig. 5, and in other instances either the pre- or the postsynaptic membrane (as in Fig. 6) may be more heavily stained. Such variations cannot necessarily be assumed to indicate quantitative differences in enzyme activity, as discussed below.

Plasma membranes of cell processes that can be identified as dendrites at areas other than synaptic sites are also well stained, whether they occur alone (Figs. 3 and 4), at dendrodendritic contacts (Fig. 7), or where they are seen arising from a perikaryon (Fig. 8); the perikaryonal membrane at these latter sites is also usually well stained. Staining at these sites was largely or totally blocked by physostigmine, in contrast to that at the ER and mitochondria of the same regions.

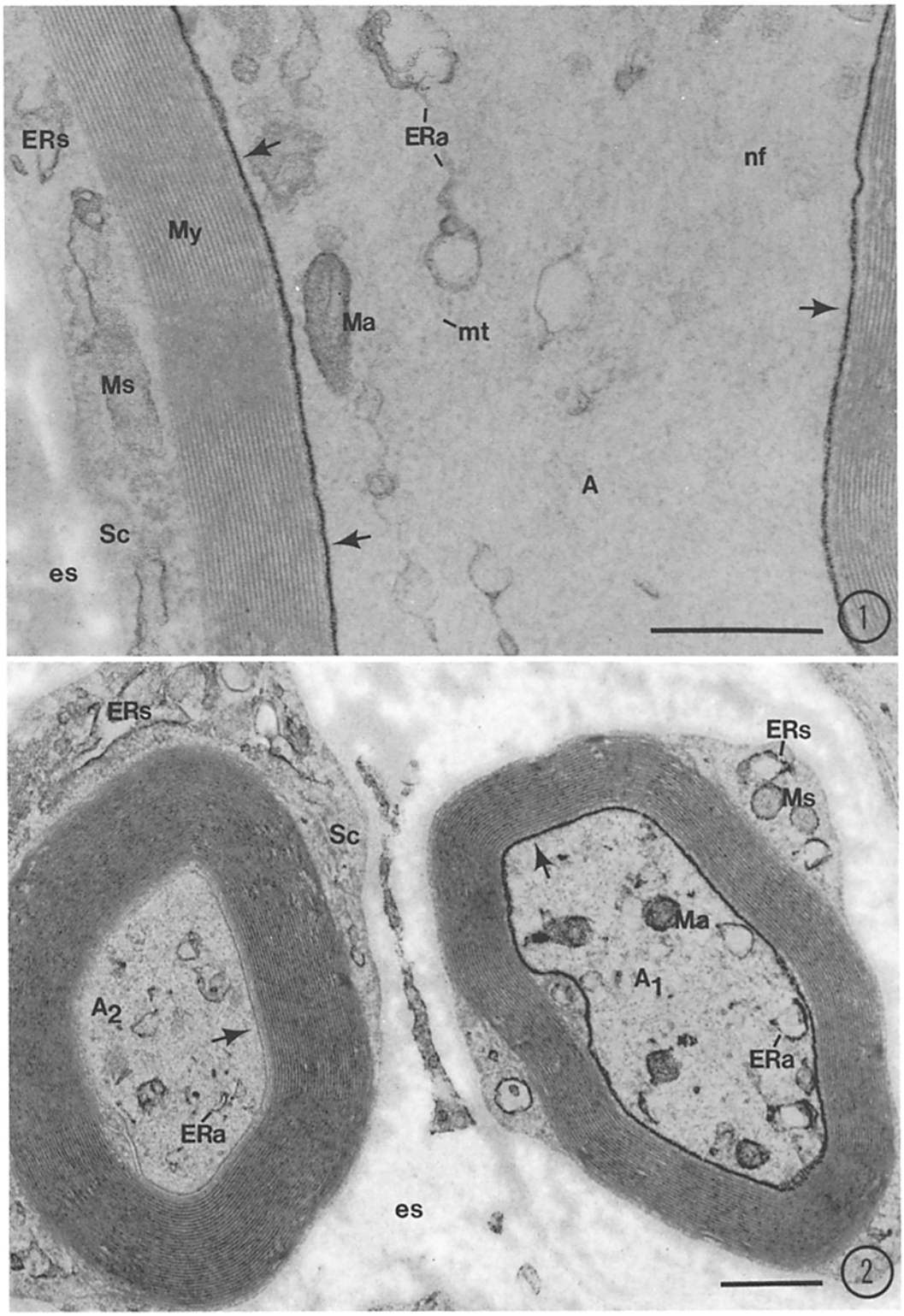
ERs
ERa
nf
My
Ma
mt
Ms
A
Sc
es
1
ERs
ERs
Ms
Sc
Ma
A1
A2
ERa
ERa
es
2

Two interesting, contrasting patterns of physostigmine-resistant staining were noted in mitochondrial membranes, for which no explanation can be offered. In near-terminal axonal varicosities (Fig. 3) and the portions involved in synaptic junctions (Figs. 5 and 6), both the inner folded and the outer mitochondrial membranes are characteristically stained. In definitely identifiable dendrites, either immediately postsynaptic (Figs. 5 and 6) or extending from a cell body (Fig. 8), and in neuronal perikarya (Fig. 8) and in Schwann cells (Figs. 3 and 6), only the outer mitochondrial membrane is generally stained. Early in the present study, it was considered that this difference is sufficiently consistent to provide a means for the tentative distinction between small axonal and dendritic cell processes found alone. On this basis, the very small neurite profile in the upper left of Fig. 3 is identified as an axon, whereas the neurites in which only the outer mitochondrial membranes are stained and which occur singly (Figs. 3 and 4) or in close contact with another similar neurite (Fig. 7) are classified as dendrites. Both patterns of mitochondrial staining persisted in the presence of physostigmine and after inactivation of AChE by sarin, as well as in sections stained for BuChE (*vide infra*).

The dendrodendritic contact illustrated in Fig. 7, both membranes of which are stained, is of the second, more highly organized type described by Elfvin (14); it shows additional faintly electron-opaque material on the cytoplasmic sides of the respective membranes (Fig. 7). These regions of specialized contact, perhaps serving as attachment plaques, are as much as 1,000 nm in length, and the contiguous plasma membranes appear more nearly straight or only gently curved as compared to membranes facing Schwann cells, and are separated by a uniform, approx. 10-nm intercellular space. As in Elfvin's report (14), it could not be distinguished whether these contacts are between cell processes of a single or of separate neurons.

Figs. 9–12 illustrate sections from iso-OMPA-treated cats that were stained in the presence of physostigmine, 3×10^{-5} M. The Au_2S deposit, therefore, represents nonspecific esterases, although minimal residual AChE or even nonenzymatic adsorption of the heavy metal ion might

---

The following symbols are the various identifying letters used in succeeding electron micrographs (Figs. 1–19):

A,	axon	*Ms,*	mitochondrion in a Schwann cell
D,	dendrite	*mt,*	microtubules
ERa,	endoplasmic reticulum in an axon	*My,*	myelin
ERd,	endoplasmic reticulum in a dendrite	*N,*	nucleus
ERs,	endoplasmic reticulum in a Schwann cell	*nf,*	neurofilaments
es,	extracellular space	*P,*	perikaryon
L,	lysosome	*rER,*	rough endoplasmic reticulum
Ma,	mitochondrion in an axon	*Sc,*	Schwann cell
Md,	mitochondrion in a dendrite	*sv,*	synaptic vesicles
Mp,	mitochondrion in a perikaryon		

FIGURES 1–8 Figs. 1–8 were stained by the $Au(TA)_2$ method, after administration of iso-OMPA in vivo to inactivate BuChE, and therefore demonstrate AChE plus nonspecific esterases.

FIGURE 1 A myelinated axon (*A*). The axolemma is intensely stained; and in favorable views (arrows) the stain is seen confined to the axolemma and not filling the intercellular space between the axolemma and the first layer of myelin (*My*). The axoplasm contains stained mitochondria (*Ma*) and membranes of vesicles and tubules of smooth ER (*ERa*), as well as unstained, faintly distinguishable neurofilaments (*nf*) and microtubules (*mt*). Schwann cell (*Sc*) cytoplasm and plasma membrane are unstained, but stain is present in Schwann cell mitochondria (*Ms*) and ER membranes (*ERs*). Extracellular space, (*es*). × 50,500. Bar, 0.5 μm.

FIGURE 2 Two myelinated axons. The axolemma (arrow) of one (A_1) is intensely stained; the axolemma (arrow) of the other (A_2) is unstained. Mitochondria (*Ma*) and elements of the ER (*ERa*) are stained within the axoplasm; these organelles (*Ms* and *ERs*) also stain within Schwann cell cytoplasm (*Sc*). Unstained are myelin sheaths, Schwann cell (*Sc*) plasma membrane and extracellular space (*es*). × 31,500. Bar, 0.5 μm.

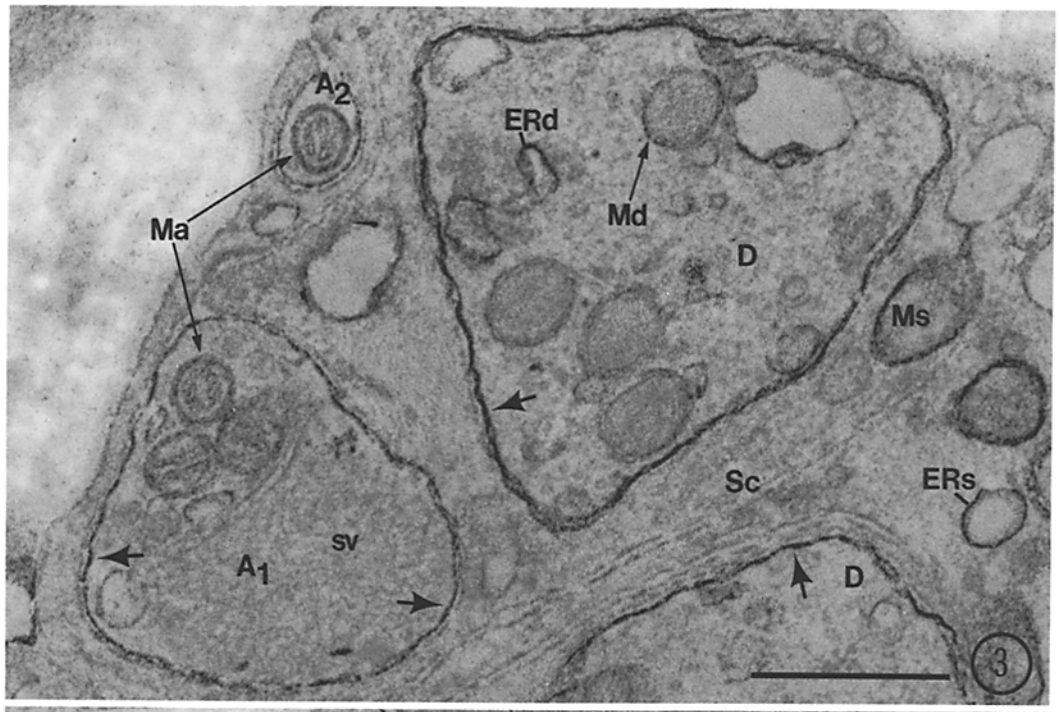
A2
ERd
Md
Ma
D
Ms
Sc
ERs
sv
A1
D
3

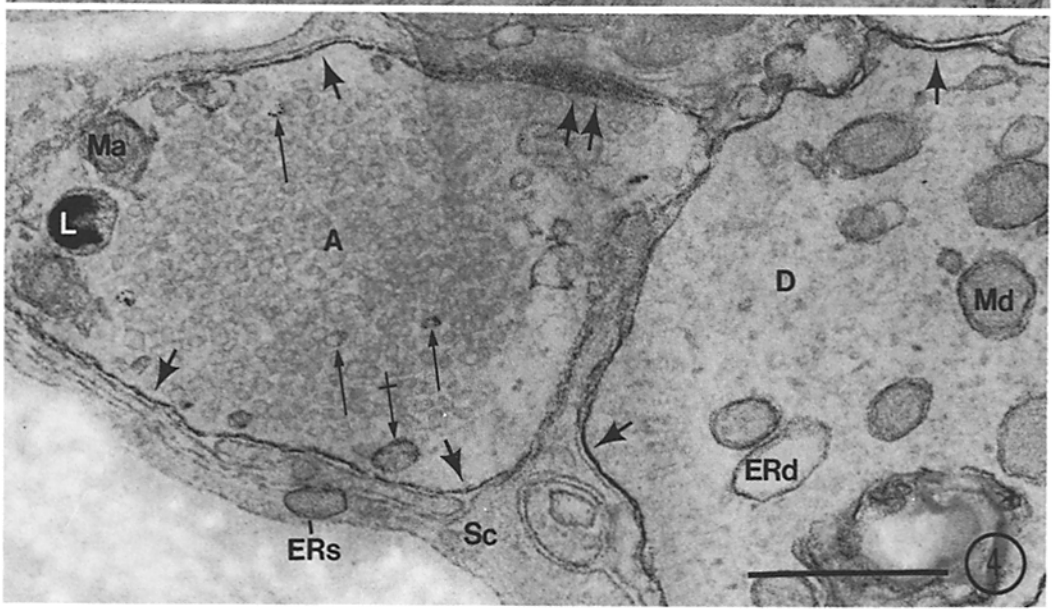
Ma
L
A
D
Md
ERd
ERs
Sc
4

also be present. It was not possible to employ controls from which the substrate was omitted, since the substrate and capturing agent are present as a single complex; the free aurous ion is not stable in aqueous solution. As mentioned above, physostigmine blocked all staining at the axolemmas of the presynaptic element wherever it could be positively identified, that is, where it is myelinated (Fig. 9), unmyelinated in near-terminal areas (Fig. 11), and at synaptic junctions (Figs. 10 and 12), indicating that essentially all of the enzymatic activity on the axolemma described above is AChE. Activity of the occasionally stained synaptic vesicles in axonal terminals was likewise prevented by physostigmine (Figs. 10–12). Dendritic (Figs. 10–12) and perikaryonal plasma membranes are usually unstained; however, an occasional dendritic (Figs. 11 and 12) or perikaryonal (Fig. 12) plasma membrane appears to retain at least a portion of its activity.

The foregoing sites at which staining is concluded to be due exclusively or predominantly to AChE are indicated diagrammatically in Fig. 20*A*.

The irregular staining of relatively light but variable intensity noted above at the membranes of the vesicular and tubular profiles of the ER in axons, Schwann cells, dendrites, and perikarya is present also in the physostigmine-treated controls (Figs. 9–12). Physostigmine-resistant staining was noted also at the perikaryonal Golgi membranes, although these structures are not included in the present figures.

Lysosomes at all sites show intense staining, both in the absence of physostigmine (Figs. 4, 6, 7, and 8) and in its presence (Figs. 10 and 11).

BuChE Staining: Cats Treated with Astra-1397 Plus Sarin in vivo for Selective Inactivation of AChE

On the basis of the criteria used here, the localization of definitely identifiable BuChE is confined to the plasma membranes of postsynaptic neuronal elements. Staining is most intense at the immediate postsynaptic sites of dendritic plasma membranes (Figs. 14–16), but extends to the remainder of the dendritic profiles and to the plasma membranes of the perikarya (Fig. 16). The pattern is also prominent at sites of dendrodendritic contact (Fig. 14). In the presence of physostigmine (Figs. 17–19), staining at all these site, but not at those noted below, was blocked or markedly reduced (Fig. 17).

In contrast with the distribution of AChE, no staining for BuChE was noted in any of the presynaptic elements, including the axolemmas of any myelinated fibers (Fig. 13), small neurites identified as terminal or near-terminal axons by their contents of synaptic vesicles (Figs. 14–16) or by the characteristic staining of both outer and inner mitochondrial membranes (Figs. 14 and 16), or in any synaptic vesicles (Figs. 14–16). Staining identifiable as BuChE is indicated diagrammatically in Fig. 20*B*.

FIGURE 3 Several neurites ensheathed by Schwann cells (*Sc*). One axon varicosity (A_1) with prominently stained axolemma (large arrows) contains numerous unstained synaptic vesicles (*sv*) and mitochondria (*Ma*) with both outer and inner folded membranes stained, while a small intervaricose region of axon (A_2) exhibits a similarly stained axolemma and a mitochondrion (*Ma*), but no vesicles. The dendrite (*D*) plasma membrane (large arrows) is also prominently stained, but its mitochondria (*Md*) exhibit staining only on the outer membrane. Intercellular spaces at axon-Schwann cell and at dendrite-Schwann cell appositions are for the most part devoid of stain. Schwann cell (*Sc*) plasma membranes are unstained, but Schwann cell mitochondria (*Ms*) are stained like dendrite mitochondria. A few membranes of the ER are stained in the dendrite (*ERd*) and also in the Schwann cells (*ERs*). × 50,500. Bar, 0.5 μm.

FIGURE 4 An axon varicosity (*A*) exhibits a stained axolemma (large arrows), and, although the vast majority of synaptic vesicles are unstained, a very few exhibit staining on the vesicle membrane (small arrows); one or two larger vesicles, resembling ER (crossed small arrow), are similarly stained. At the upper center of the figure (double large arrow), what appears as an exceptionally wide axon-Schwann cell interspace filled with endproduct is probably due to an abrupt curving of the axolemma to a direction parallel to the plane of section, or, alternatively, to fragmenting and smearing of the endproduct during sectioning. A dendrite (*D*) which is in contact with the axon also exhibits a well stained plasma membrane (large arrow) and characteristically stained outer mitochondrial membranes (*Md*). Schwann cells (*Sc*) are unstained except for a few vesicles of ER (*ERs*). Other stained structures include a vesicle of ER in the dendrite (*ERd*) and a mitochondrion (*Ma*) and a lysosome (*L*) in the axon. × 50,500. Bar, 0.5 μm.

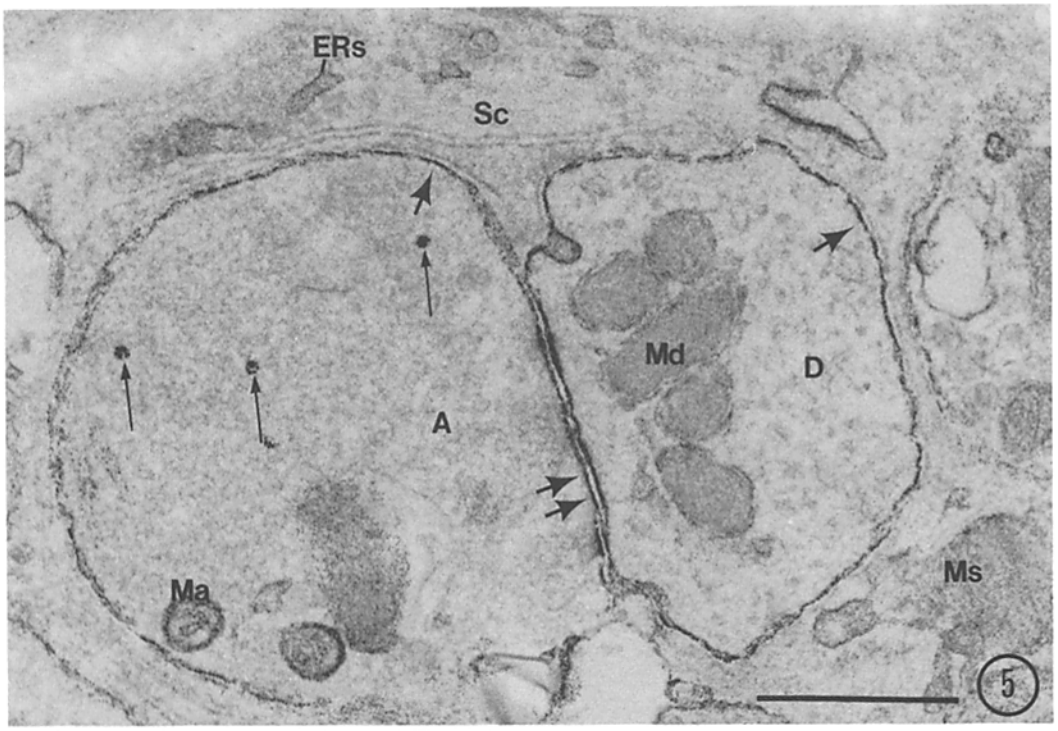
ERs
Sc
Md
D
A
Ma
Ms
5

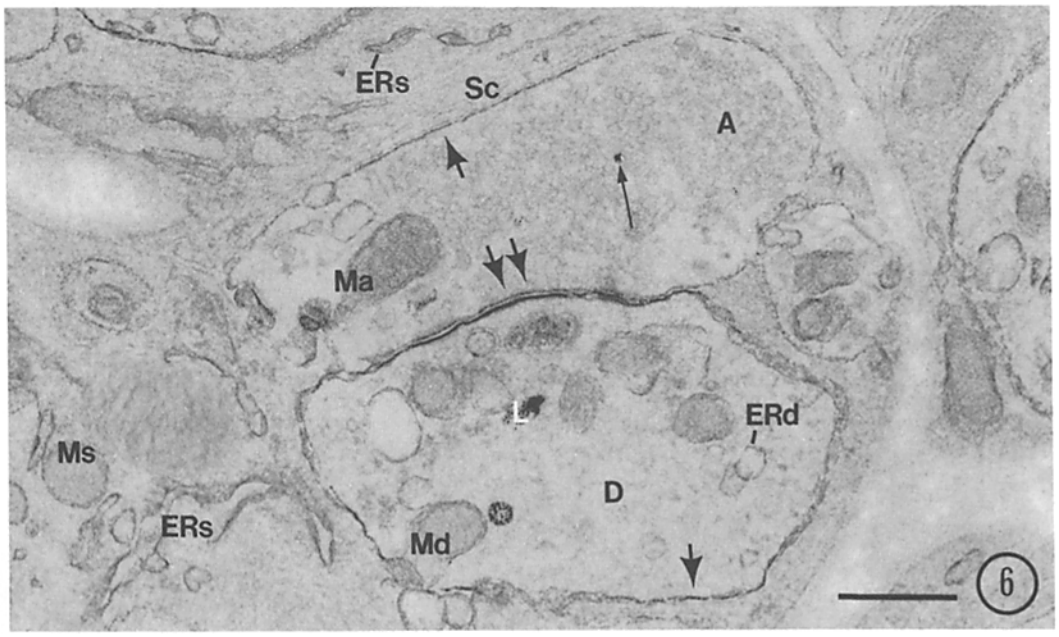
ERs
Sc
A
Ma
ERd
Ms
D
ERs
Md
6

As with tissues stained for AChE, ER membranes of axons, dendrites, ganglion cell perikarya, and Schwann cells were stained irregularly both in the absence (Figs. 13–16) and in the presence (Figs. 17–19) of physostigmine. The same two contrasting patterns of physostigmine-resistant mitochondrial staining (i.e., inner as well as outer mitochondrial membranes stained only at presynaptic axonal sites) were noted here as in tissues from iso-OMPA-treated cats, as was intense staining of lysosomes. Again, no staining was detected in this series at axonal neurofilaments or microtubules or at Schwann cell plasma membranes.

DISCUSSION

The $Au(TA)_2$ method has been demonstrated in the accompanying electron micrographs to localize enzymatic activity by a finely granular, electron-opaque precipitate of Au_2S. At membranous sites, the deposit is generally even and continuous rather than patchy in distribution, with little extension into intercellular spaces, suggesting that diffusion of the reaction product is minimal. The crisp staining of the axolemmas of myelinated fibers as well as numerous intracellular structures indicates that the $[Au(TA)_2]^-$ complex penetrates formalin-fixed tissue satisfactorily to a distance beyond 200 μm from the surface. The principal limitation of the method is its lack of specificity, but for AChE and BuChE this has been overcome to a considerable extent by the employment of appropriate combinations of selective inhibitors in vivo and in vitro, and by the concomitant staining of sections for LM examination by the CuThCh method.

The now voluminous literature on the fine structural localization of cholinesterases has been partially reviewed recently (9, 46, 63, 68), and only those aspects that are most pertinent to the present findings will be cited here.

Most of the AChE in the cat SCG appeared to be confined to neuronal plasma membranes, both pre- and postsynaptic, whereas the localization of BuChE was restricted chiefly to the latter site, as depicted in Fig. 20. The AChE-stained presynaptic axon could be identified positively only where it was myelinated, approaching a synaptic contact, or actually involved in a synaptic junction. It is inferred from these findings that the axolemma of the unknown or unidentified segment between the myelinated portion and the synaptic endings is probably also endowed with AChE. Likewise, although our account of dendritic branches of various sizes and in various relationships is more completely illustrated, we still are inferring from these isolated views that probably the entirety of dendritic membranes and also those of the perikaryon from which they arise possess both AChE and BuChE. Further, since the enzyme activity on the axolemma was resistant to iso-OMPA but inactivated completely by physostigmine, the axolemma does not appear to possess a significant concentration of either BuChE or nonspecific esterase. On the other hand, the activity on the plasma membrane of the postsynaptic cell and its dendrites is comprised primarily of AChE and BuChE, but may include also some nonspecific

FIGURE 5 An axodendritic synapse with plasma membranes (large arrows) of both the axon (*A*) and dendrite (*D*) entirely stained, perhaps slightly more heavily at the site of axodendritic contact (double large arrows). The intervening synaptic cleft, however, as well as other intercellular spaces between the neurites and adjacent Schwann cells (*Sc*), are unstained. Among the numerous unstained synaptic vesicles in the axoplasm, a few vesicles (small arrows) appear to be filled with reaction product. Axonal mitochondria (*Ma*) are stained on both outer and inner folded membranes, whereas mitochondria of the dendrite (*Md*) and Schwann cells (*Ms*) are stained almost exclusively on the outer membrane. A few stained tubules of ER (*ERs*) are also present in the Schwann cells. × 50,500. Bar, 0.5 μm.

FIGURE 6 An axodendritic synapse in which the dendrite (*D*) plasma membrane appears more densely stained than that of the axon (*A*) both at the area of synaptic contact (double large arrows) and at areas facing unstained Schwann cell (*Sc*) plasma membranes (single large arrows). The synaptic cleft and other intercellular spaces are unstained. One small vesicle (small arrow) and a mitochondrion (*Ma*) are stained within the axoplasm. Mitochondria of the dendrite (*Md*) and Schwann cell (*Ms*) are stained on their outer membranes. Other structures stained include ER membranes of the dendrite (*ERd*) and Schwann cells (*ERs*), and lysosomes (*L*) within the dendrite. × 31,500. Bar, 0.5 μm.

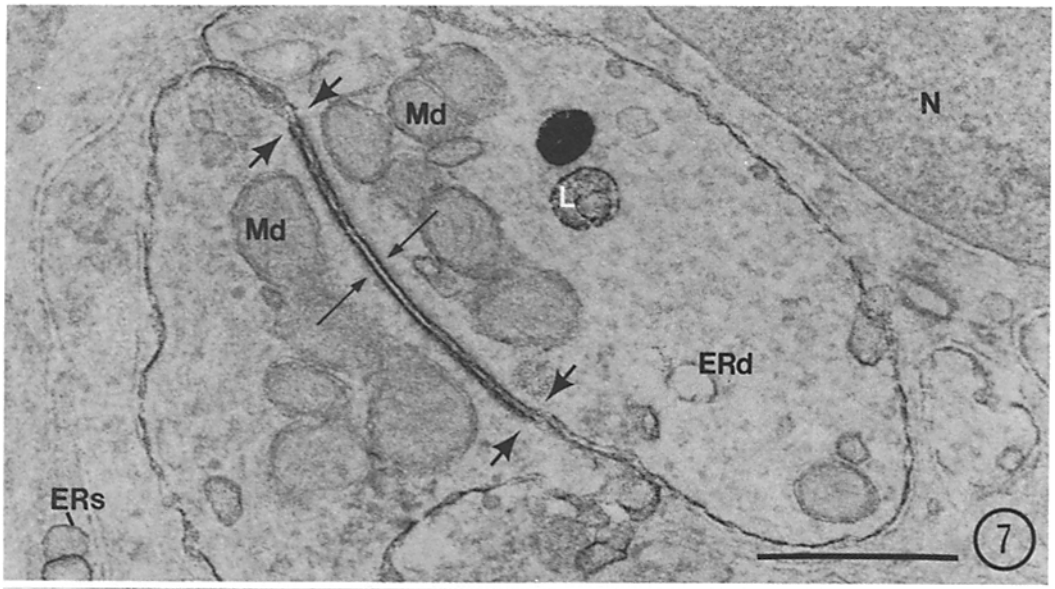
Md
N
L
Md
ERd
ERs
7

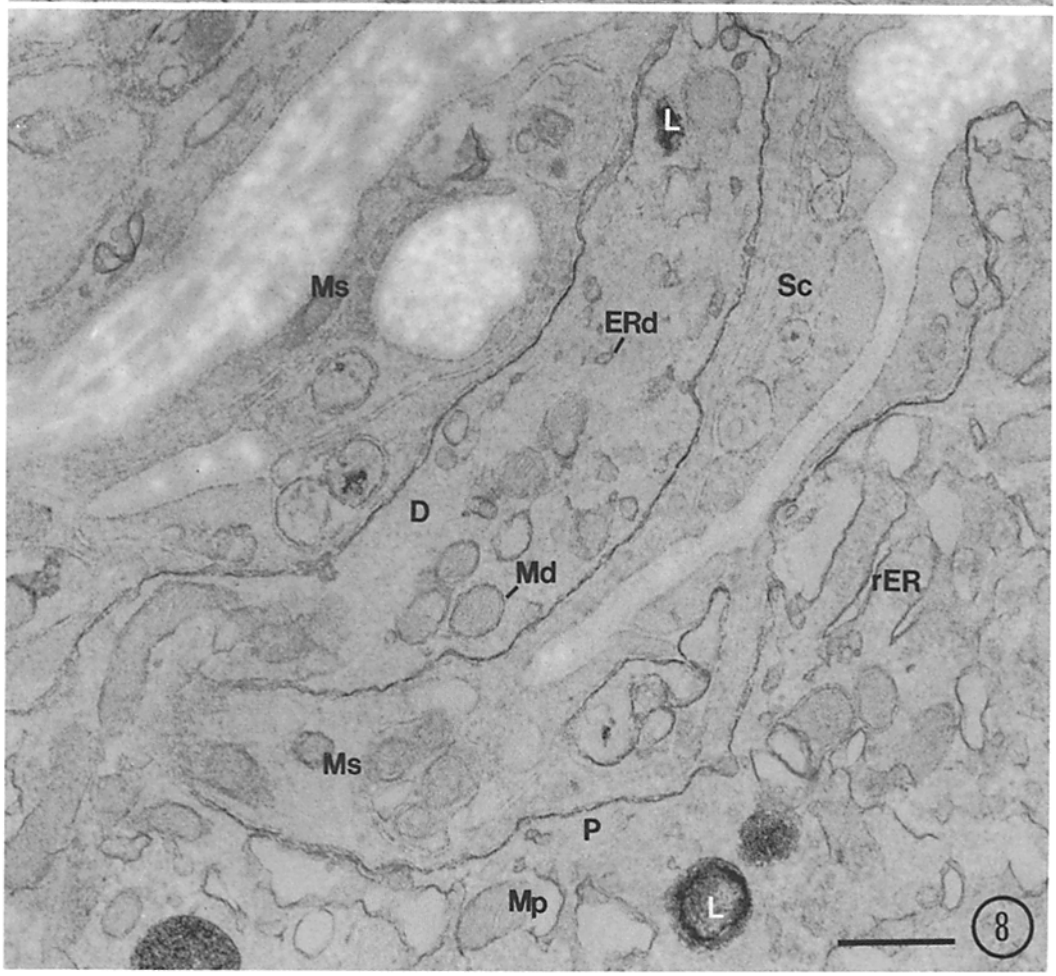
L
Ms
Sc
ERd
D
Md
rER
Ms
P
Mp
L
8

esterase, since it was not always entirely inactivated by physostigmine. In previous EM demonstrations of AChE in the SCG of the rat (24, 27) and frog (6, 67), in which modifications of the CuThCh method were employed, most of the enzymatic activity was localized within the clefts between the pre- and postsynaptic membranes. The difference in localization with the latter methods is probably due chiefly to the coarser dimensions and lower electron opacity of the reaction product, and possibly its diffusion or translocation before precipitation. This is reflected also in most previous descriptions of AChE-staining of axonal membranes, where the precipitate was generally found to fill the axolemmal-Schwann cell interspace (6, 47, 67, 68).

The only additional site where staining could be definitely attributed to AChE, since it was blocked by physostigmine, was in occasional synaptic vesicles. This pattern differs from that noted previously with the lead-thiolacetic acid method after brief OsO_4 prefixation at the neuromuscular junction, where nearly all of the vesicles were stained but probably not due to AChE, since staining persisted after treatment with paraoxon (1). The present finding suggests the interesting possibility that in the recycling of the vesicular membrane components by endocytosis, as proposed by Heuser and Reese (22), the underlying mechanism makes an occasional error in membrane recognition and includes a portion of the AChE-containing axolemmal component. However, if this should occur to a significant extent, the AChE-content of the vesicular and axolemmal membranes should eventually be randomized. Alternatively, the AChE-stained vesicles may represent transport vesicles derived from the ER, as discussed below.

At sites where staining persisted in physostigmine-treated controls, indicating the presence of other esterases or possibly nonenzymatic adsorption of $[Au(TA)_2]^-$ or a breakdown product, the additional presence of AChE or BuChE can not be excluded. Comparative intensities of staining at various sites afford only a rough approximation of relative enzyme concentrations. Consequently, there might be no discernible difference between staining produced by a nonspecific esterase plus a relatively low concentration of AChE or BuChE in one section and that observed in a comparable physostigmine-treated control in which the activity of AChE or BuChE had been suppressed. Thus, for example, the present results are not inconsistent with reports of staining for AChE at elements of the smooth ER of cholinergic axons by means of modifications of the more specific CuThCh method (9, 26, 28). The presence of AChE at such sites might be expected, in keeping with early proposals that most of the enzyme is synthesized in the rough ER of the perikaryon and then transported to the axonal terminals via the smooth ER (40, 44, 48). More recent evidence has indicated that approx. 15% of the total axonal AChE is in the process of rapid transport, two-thirds in the forward and one-third in the retrograde direction, and that the remainder is divided between the fixed and slowly transported fractions (49, 54, 59, 64). The site of the rapid transport fraction is uncertain; it has been assigned to the smooth ER (12) and, alternatively, to the axonal microtubules and/or neurofilaments in association with hypothetical transport filaments to which the rapidly

FIGURE 7 A dendrodendritic contact of the complex type where the stained contiguous plasma membranes appear as rigidly parallel lines about 9 nm thick separated by an unstained intercellular space of about 10 nm, with additional faintly opaque material (small arrows) on the cytoplasmic surfaces of the associated membranes. The length of complex membrane apposition between the pairs of large arrows is nearly 1000 nm; dendrite plasma membranes continuous with this segment, and in simple apposition, are also stained. Other structures stained include dendrite mitochondrial outer membranes (*Md*), ER membranes (*ERd*) and lysosomes (*L*), and some Schwann cell ER membranes (*ERs*). A Schwann cell nucleus (*N*) is also labeled. × 50,500. Bar, 0.5 μm.

FIGURE 8 A well stained plasma membrane is present both on the perikaryon (*P*) and on a small dendritic branch (*D*) issuing from it. Mitochondria of the dendrite (*Md*), perikaryon (*Mp*), and Schwann cell (*Ms*) exhibit staining on the outer membrane only. Some staining is present on membranes of the rough ER (*rER*) of the perikaryon; it can not be distinguished whether the stained ER membranes in the dendrite (*ERd*) are rough or smooth. Other structures labeled include Schwann cell cytoplasm (*Sc*) and lysosomes (*L*). × 31,500. Bar, 0.5 μm.

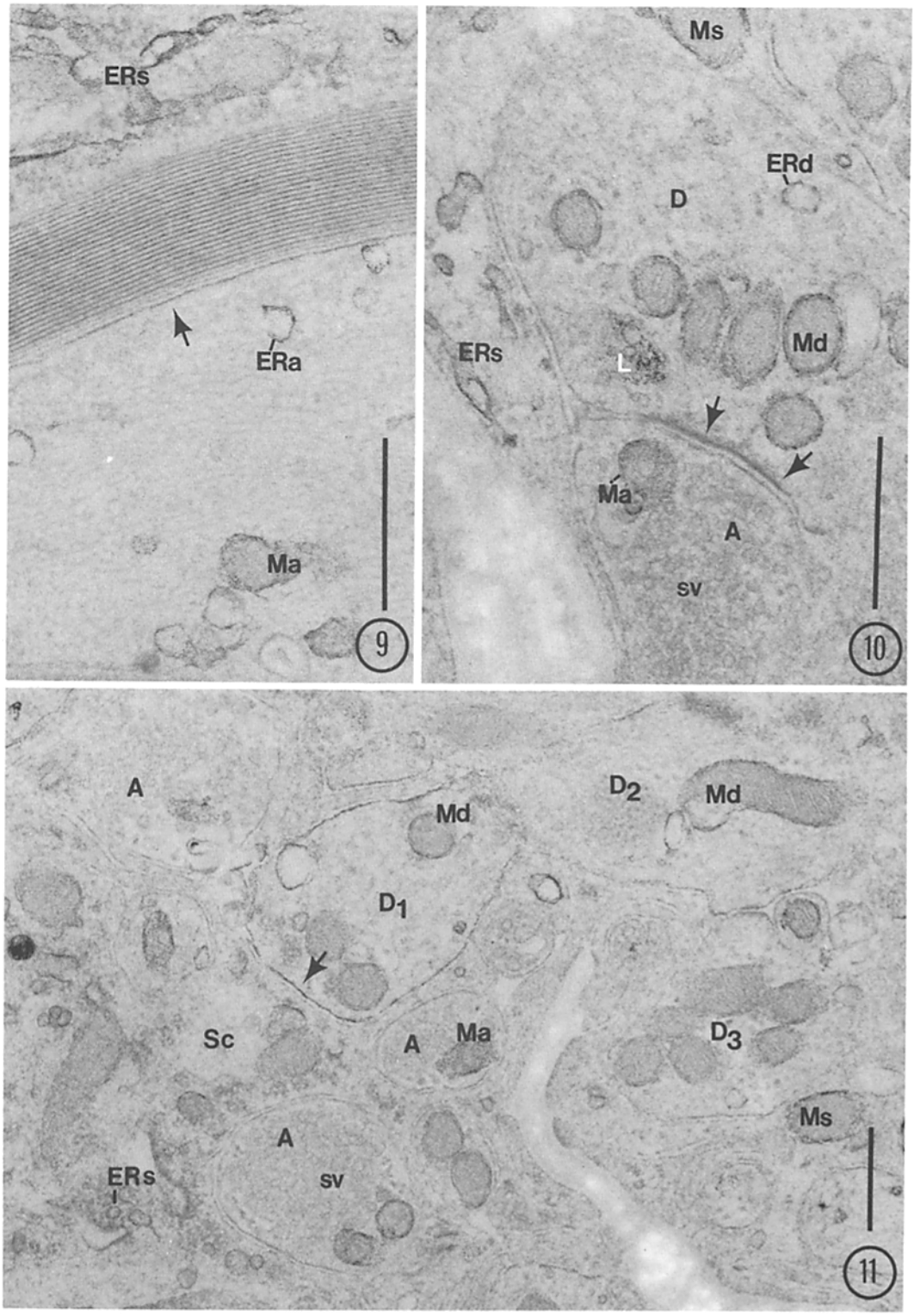
ERs
ERa
Ma
9
Ms
ERd
D
ERs
L
Md
Ma
A
sv
10
A
Md
D2
Md
D1
Sc
A
Ma
D3
Ms
A
ERs
sv
11

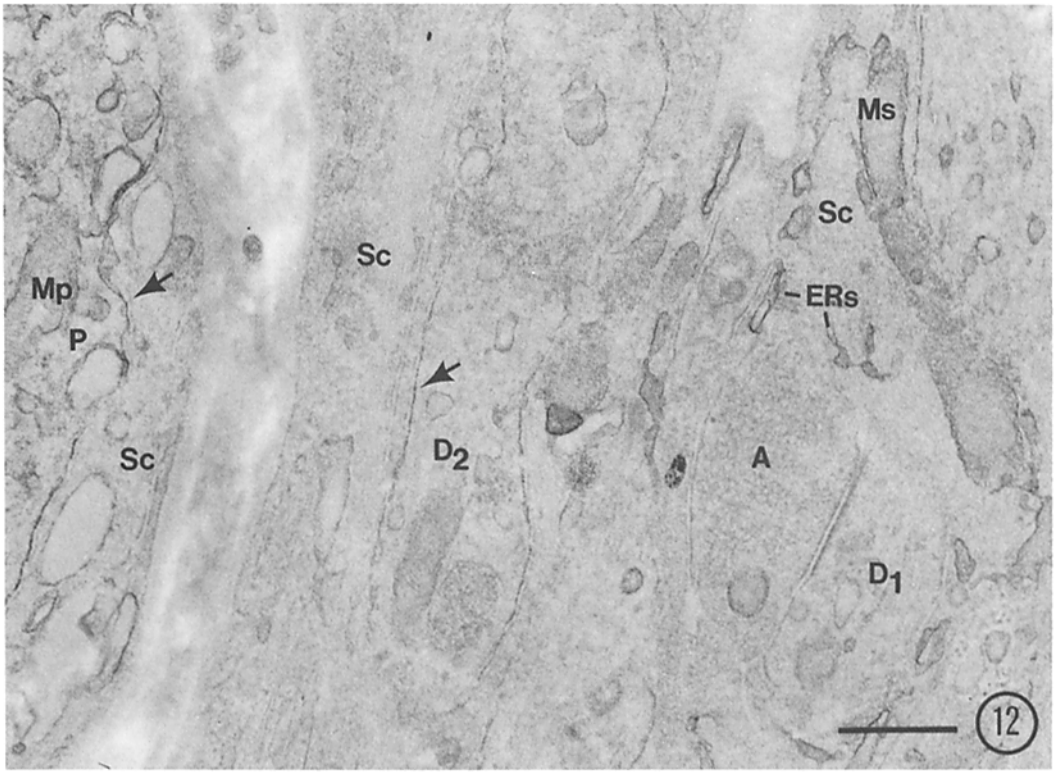

FIGURE 12 An axon terminal (*A*) in synaptic contact with a dendrite (D_1), both having unstained plasma membranes. However, another dendrite (D_2) and a perikaryon (*P*) exhibit some residual staining on their plasma membranes (arrows). Mitochondria (*Mp*) and other membranous structures in the perikaryon are also moderately stained. In one area of Schwann cell cytoplasm, ER membranes (*ERs*) and mitochondria (*Ms*) are markedly stained; in other areas, they are unstained. × 31,500. Bar, 0.5 μm.

FIGURES 9–12 Figs. 9–12 were stained by the $Au(TA)_2$ method after administration of iso-OMPA in vivo, followed by physostigmine in vitro; they therefore demonstrate only nonspecific esterases, minimal residual AChE, and any metal ion adsorption.

FIGURE 9 A myelinated axon after physostigmine inactivation of AChE exhibits stained axoplasmic mitochondria (*Ma*) and smooth ER membranes (*ERa*) and also Schwann cell ER membranes (*ERs*), about the same as in Figure 1. Unstained, however, is the axolemma (arrow). × 50,500. Bar, 0.5 μm.

FIGURE 10 The plasma membranes of a small axon terminal or varicosity (*A*) and a dendrite (*D*) in synaptic contact are completely devoid of stain, even at the postsynaptic membrane thickening (arrows). ER membranes of the dendrite (*ERd*) and Schwann cell (*ERs*) are stained, as are the outer mitochondrial membranes in both dendrite (*Md*) and Schwann cell (*Ms*), and a lysosome (*L*). Synaptic vesicles (*sv*) within the axoplasm are unstained, but a mitochondrion (*Ma*) shows some staining. × 50,500. Bar, 0.5 μm.

FIGURE 11 Profiles of three axon varicosities (*A*) exhibit unstained axolemmas and synaptic vesicles (*sv*), but characteristically stained mitochondria (*Ma*). The plasma membrane of one dendrite (D_1) shows some residual staining (arrow), while the plasma membranes of two other dendritic profiles (D_2 and D_3) are unstained. Some of the mitochondria of the dendrites (*Md*) and of a Schwann cell (*Ms*) show staining of the outer membrane only; others are practically unstained. Schwann cell cytoplasm (*Sc*) also contains some lightly stained ER membranes (*ERs*). × 31,500. Bar, 0.5 μm.

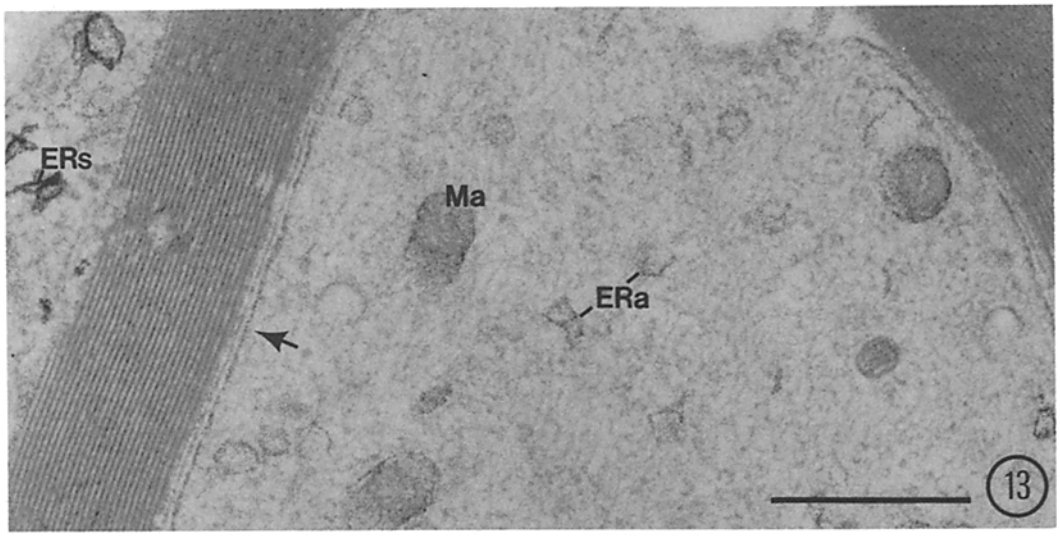
ERs
Ma
ERa
13

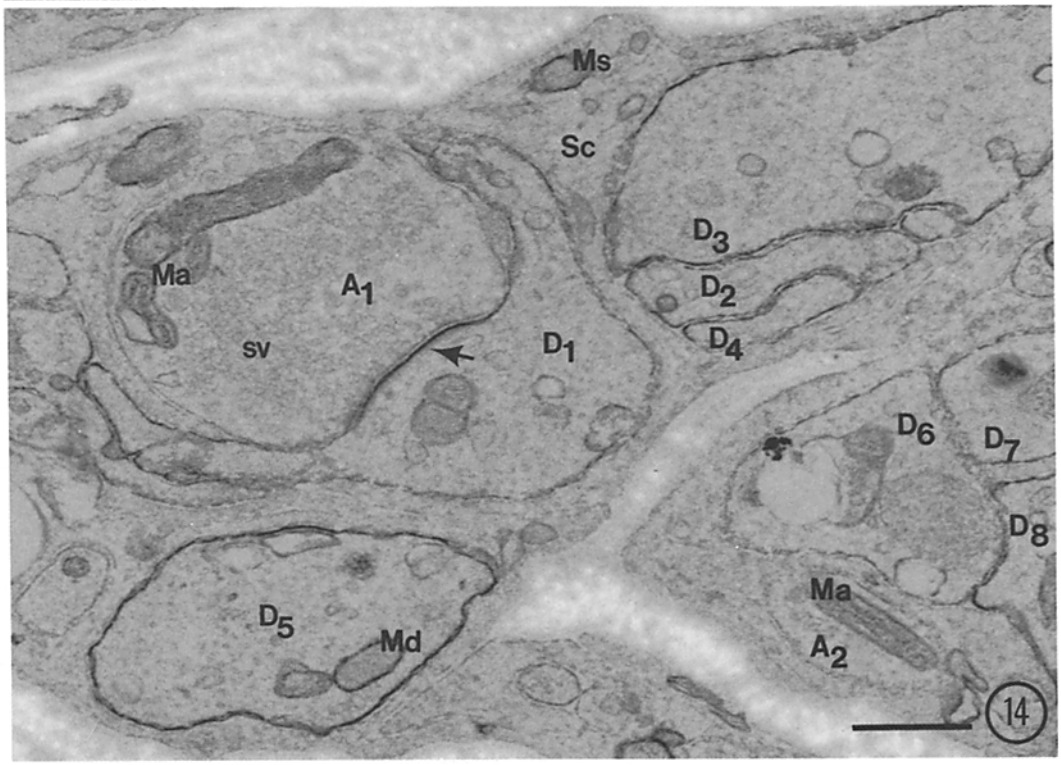
Ms
Sc
D3
D2
D4
Ma
A1
sv
D1
D6
D7
D8
Ma
A2
D5
Md
14

moved components are postulated to be bound (54, 55). In either case, the localization of this fraction may have been partially obscured here by the presence of other esterases, as mentioned, lost because of high diffusibility with inadequate fixation, or missed because its concentration is below the threshold detectable by the present method. The intense AChE staining of the axolemmas of most of the myelinated fibers focuses attention there as the probable major site of fixed AChE and perhaps of part of the slowly transported AChE as well. The concept of a continuously elongating sleeve of enzyme for eventual use at the axonal terminal (63) is not inconsistent with the original proposal of Weiss and Hiscoe (66), that axoplasmic flow represents the perpetual longitudinal growth of the entire axon. A substantial body of evidence (32, 63) weighs against the hypothesis that the AChE of the axolemma participates in impulse conduction (53).

Although it has not been demonstrated directly here that unmyelinated and myelinated postganglionic axonal membranes are devoid of AChE activity, it is reasonable to infer that this is so. The definite identification of postganglionic axons in the SCG is complicated by the fact that most of them probably arise from dendrites, and hence, in EM sections, cannot be related directly to their ganglion cells of origin (11, 14). The occasionally noted, unstained myelinated axons are probably in most cases postganglionic rather than afferent (3, 60); as will be described in a subsequent report, such fibers persisted after preganglionic denervation. In LM studies of the cat SCG stained by the more specific CuThCh method, the fibers of the preganglionic trunk are stained intensely, whereas those of the major postganglionic internal carotid trunk and the smaller branches are unstained (29, 31). This has been corroborated by EM observations of the AChE-stained cat nictitating membrane, in which less than 0.5% of the nearly exclusively adrenergic fibers that originate from the SCG was stained (19).

It is doubtful that the variable degrees of physostigmine-resistant staining noted at the mitochondria represent significant amounts of AChE or BuChE. Staining of these organelles by the lead thiolacetic acid method has been reported for a variety of tissues (2). While no reason can be offered for the difference noted consistently between the staining of mitochondria in identifiable preganglionic axons and their terminals, where the inner as well as the outer mitochondrial membranes were stained, and in dendrites and elsewhere (staining of outer membrane only), this feature appears to offer a useful if empiric means of distinguishing between isolated axonal and dendritic processes, at least in the cat SCG. Preganglionic denervation (as will be reported in detail in a succeeding publication) results in the loss of all myelinated axons with AChE-positive axolemmas, while allowing a number of AChE-negative axons to persist; hence, the AChE-positive axons are identified here as presynaptic, while the unstained axons, which remain after denervation, probably represent the myelinated postsynaptic axons referred to in Results. Denervation also removes all small neurites (with and without clus-

FIGURES 13–16 Figs. 13–16 were stained by the $Au(TA)_2$ method, after administration of Astra 1397/sarin in vivo to inactivate AChE, and therefore demonstrate BuChE plus nonspecific esterases.

FIGURE 13 A myelinated axon showing some staining of mitochondrial (*Ma*) and ER membranes (*ERa*), but an unstained axolemma (arrow). Within the Schwann cell some ER membranes (*ERs*) are also stained. × 50,500. Bar, 0.5 μm.

FIGURE 14 An axon terminal (A_1), with unstained axolemma and synaptic vesicles (*sv*) but with characteristically stained inner and outer mitochondrial membranes (*Ma*), is in synaptic contact with a dendrite (D_1) exhibiting a completely stained plasma membrane, particularly at the postsynaptic thickening (arrow). A small neurite (A_2) at the lower right with unstained plasmalemma, but with lightly stained inner and outer mitochondrial membranes (*Ma*), is probably a near-terminal axon. A dendrite (D_2) is in simple, close appositional contact with two other dendrites (D_3 and D_4); all of their plasma membranes are stained. Still another isolated neurite profile (D_5) with a prominently stained plasmalemma is identified as a dendrite on the basis of the characteristic staining pattern of its mitochondria (*Md*), namely the prominent staining of the outer membrane but virtual absence of staining from the folded inner membrane. Other small neurites such as D_6, D_7, and D_8 with moderately stained plasmalemmas but without visibly stained mitochondria are also probably dendrites. Little is stained in the Schwann cells (*Sc*) except for outer mitochondrial membranes (*Ms*). × 31,500. Bar, 0.5 μm.

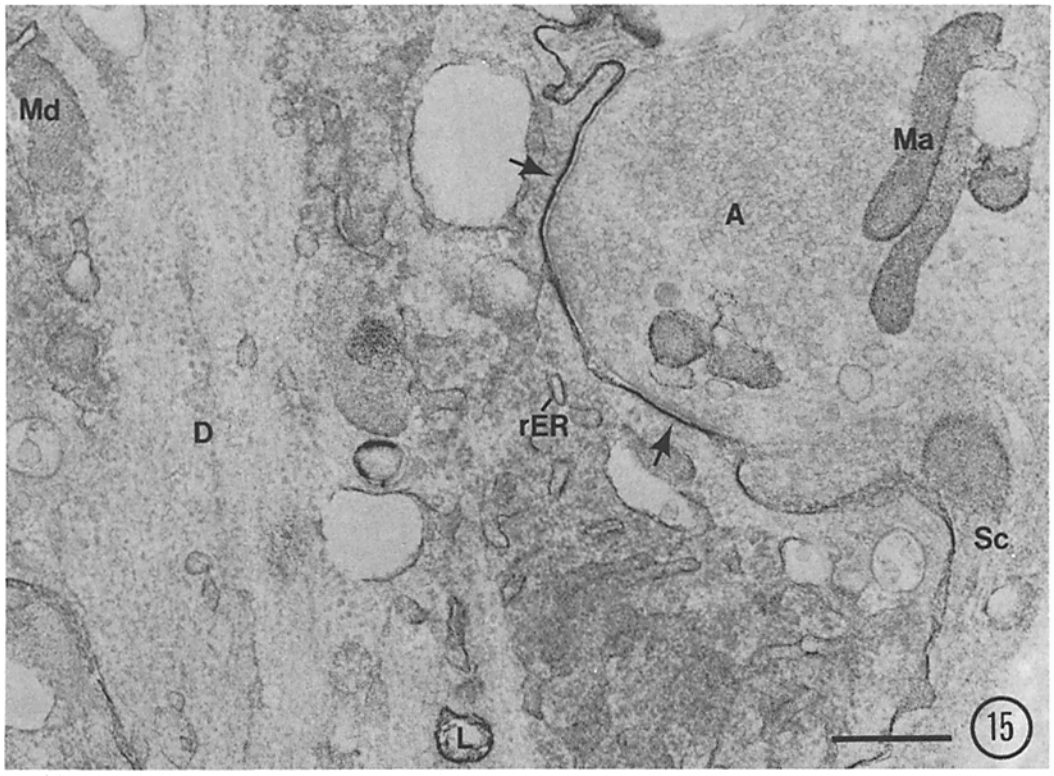
Md
Ma
A
D
rER
Sc
L
15

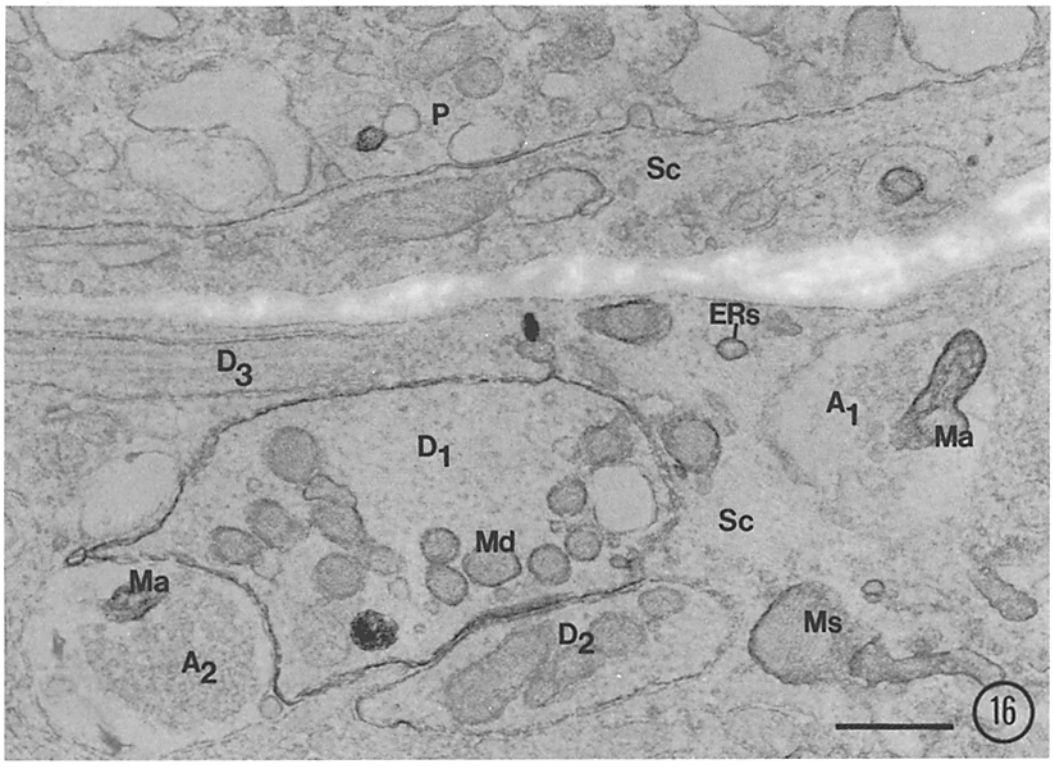
P
Sc
ERs
D3
A1
Ma
D1
Sc
Md
Ma
Ms
D2
A2
16

ters of synaptic vesicles) that contain mitochondria with stained outer and inner membranes. The small neurites that remain after denervation consistently exhibit mitochondria with only the outer mitochondrial membranes stained. For these reasons, the differential nonspecific staining of mitochondrial membranes appears consistent with our interpretation. Lysosomes likewise stained intensely in the presence of physostigmine; similar staining with the lead thiolacetic acid method has been attributed to a C-esterase (65).

In view of the very small population of cholinergic ganglion cells in the cat SCG, where in accordance with LM observations intense staining of the rough ER would be expected, it is not surprising that none was noted. Similarly, no structures identifiable as SIF cells were found. On the other hand, the light, physostigmine-resistant staining for both AChE and BuChE noted consistently in the rough ER of the perikarya of ganglion cells, as at other sites, is consistent with the possibility discussed below that these enzymes as well as other esterases are synthesized postsynaptically for distribution to the dendritic and perikaryonal membranes.

As stated in the introduction, the cytological distributions of both enzymes noted here by direct EM observation are markedly different from those deduced from LM and quantitative studies in which normal and denervated ganglia were compared. The first of these is the extensive postsynaptic neuronal distribution of AChE. This indicates that the loss of practically all the AChE from the neuropil within a few days after preganglionic denervation (the confirmation of which by EM observation will be described in a subsequent publication) must be attributed to factors other than degeneration of its original site of localization. One possibility is that AChE is released continually by the presynaptic terminals, then migrates through the interneuronal and dendrite-Schwann cell interspaces to become incorporated on the dendritic and perikaryonal membranes at a relatively rapid turnover rate (9, 51). Two of the present observations seem inconsistent with this explanation: the extensive, uniform localization of postsynaptic AChE at sites far removed from contact with presynaptic terminals, and the absence of significant staining within the clefts. As at certain intraaxonal sites, we can not exclude at present the possibility that AChE occurs within the clefts in a highly diffusible form or at a concentration below the threshold for staining. However, studies with radioactively labeled proteins have indicated that the transfer of macromolecules across synapses is a limited process (13). A more tenable hypothesis is that a trophic factor, released by the presynaptic terminals, is essential for the synthesis of AChE by the postsynaptic neurons. This possibility is now being explored.

The second unexpected finding is the localization of most of the ganglionic BuChE at postsynaptic neuronal membranes, where its distribution resembles that of AChE, rather than at the plasma membranes of Schwann cells as concluded previously. The earlier conclusion was based on the slow, limited decline in ganglionic BuChE after sectioning of the preganglionic trunk, cited above, and some related observations: the apparent restriction of BuChE in the dorsal root and ciliary ganglia (29) and in the brain (5, 61) of the cat to

FIGURE 15 An axon terminal (*A*) with unstained axolemma and synaptic vesicles, but with stained mitochondria (*Ma*), making synaptic contact with a large dendrite (*D*) whose plasma membrane is intensely stained at the postsynaptic site (arrows) and also at areas facing Schwann cells (*Sc*). Within the dendrite, membranes of rough ER (*rER*), mitochondria (*Md*), and a lysosome (*L*) show some staining. × 31,500. Bar, 0.5 μm.

FIGURE 16 A small axon profile (A_1) occurs alone, while another (A_2) is in synaptic contact with a dendrite (D_1) which in turn is in simple appositional contact with another dendrite (D_2). Both axons (A_1 and A_2) exhibit unstained axolemmas and synaptic vesicles, but characteristically stained inner and outer mitochondrial membranes (*Ma*). The dendrites (D_1 and D_2) show stained plasma membranes and either lightly stained mitochondria as in D_2 or distinctively stained outer mitochondrial membranes (*Md*) as in D_1. A small neurite (D_3), with lightly stained plasmalemma but without visible mitochondria to aid in its identification, is probably also a dendrite. At the top of the figure, a perikaryonal (*P*) plasma membrane is moderately stained, although the perikaryonal intracellular membranes are for the most part unstained. Some mitochondrial outer membranes (*Ms*) as well as ER vesicles (*ERs*) are stained within the Schwann cell cytoplasm (*Sc*). × 31,500. Bar, 0.5 μm.

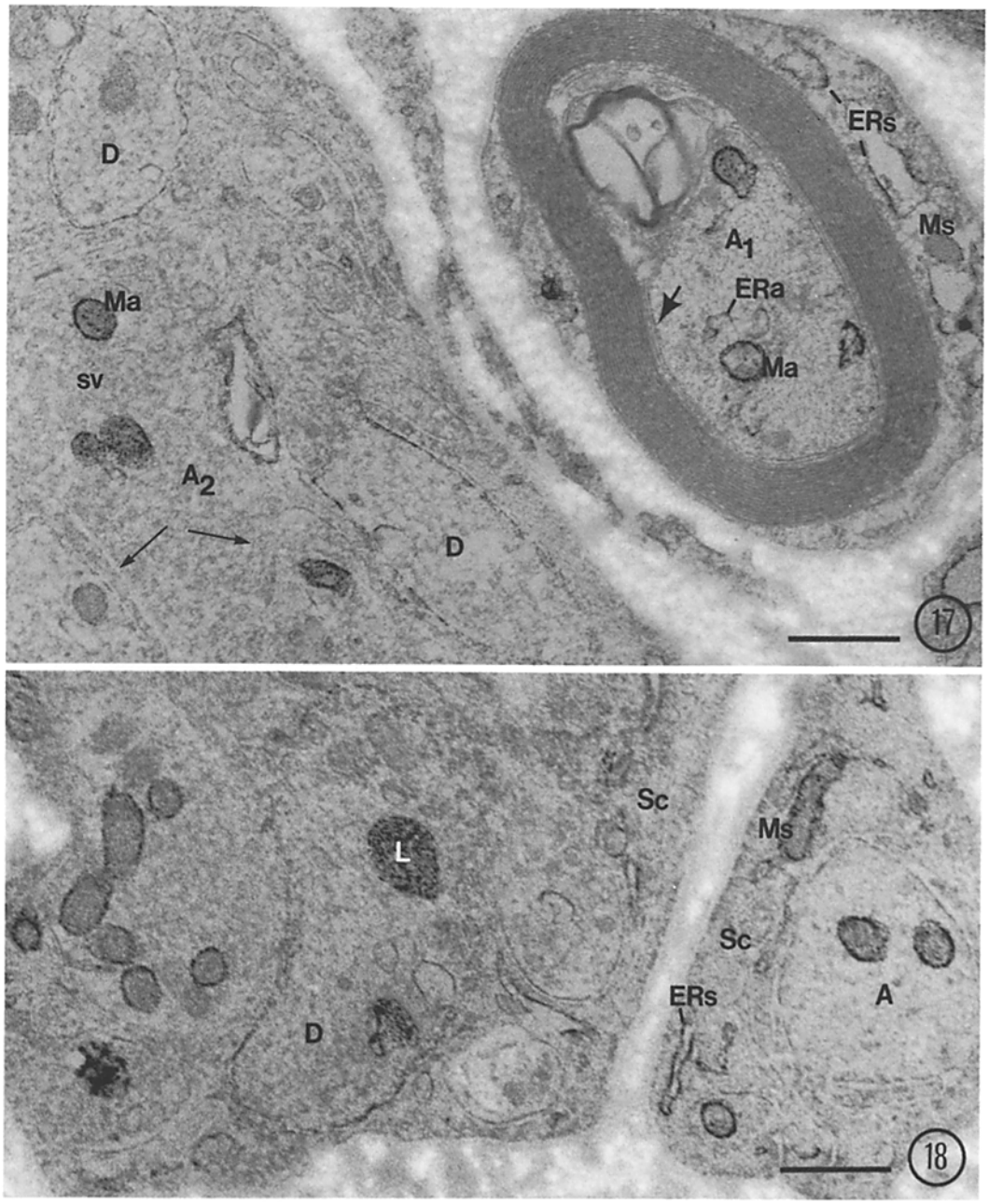

FIGURES 17–19 Figs. 17–19 were stained by the $Au(TA)_2$ method after Astra 1397/sarin in vivo, followed by physostigmine in vitro; they therefore demonstrate only nonspecific esterases, minimal residual BuChE, and any metal ion adsorption.

FIGURE 17 To the right is a myelinated axon (A_1) with unstained axolemma (large arrow) but with stained mitochondria (*Ma*) and ER membranes (*ERa*). The adjacent Schwann cell also shows some staining in its mitochondria (*Ms*) and ER membranes (*ERs*). To the left a small unmyelinated axon (A_2), containing remnants of synaptic vesicles (*sv*), shows a faintly discernible unstained axolemma (small arrows) and characteristically stained inner and outer mitochondrial membranes (*Ma*). Two neurites (*D*) which show slight residual staining on the plasma membranes are probably dendrites. × 31,500. Bar, 0.5 μm.

FIGURE 18 A group of neurites that are practically unidentifiable. One containing stained lysosomes (*L*) and a lightly stained plasma membrane is probably a dendrite (*D*). Another process with unstained plasma membranes but with deeply stained mitochondria is probably an axon (*A*). Schwann cells (*Sc*) are unstained except for prominently stained mitochondria (*Ms*) and ER membranes (*ERs*). × 31,500. Bar, 0.5 μm.

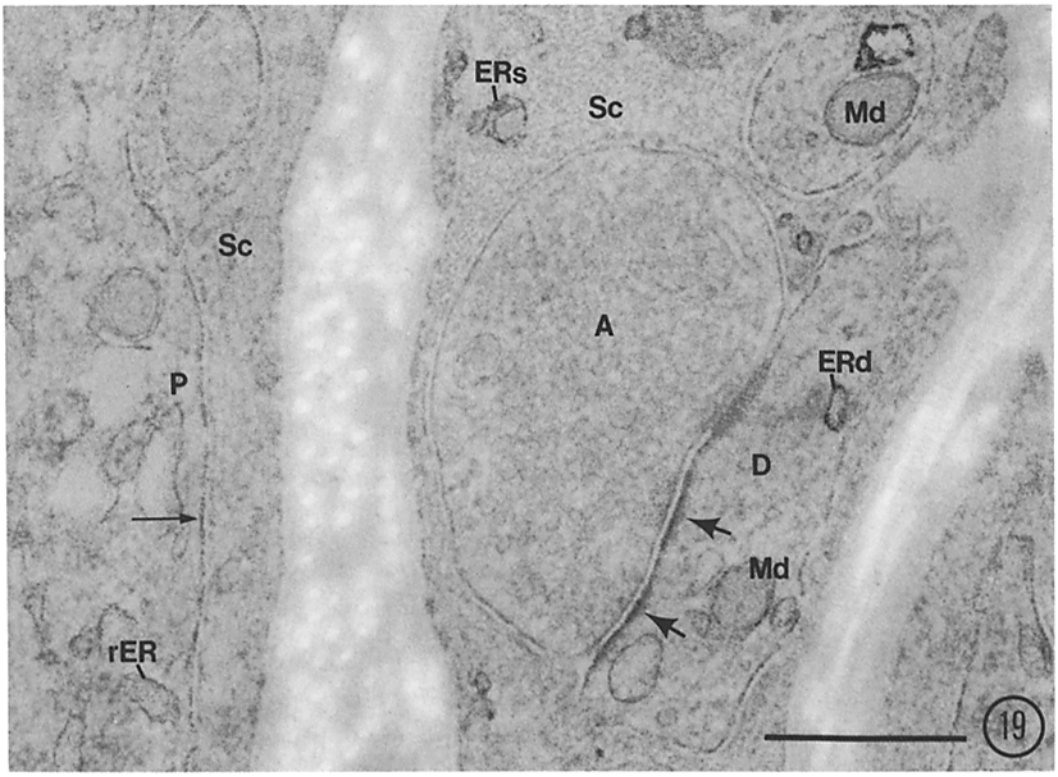

FIGURE 19 An axodendritic synapse in which the axonal (*A*) plasma membrane and synaptic vesicles are devoid of stain. The thickened postsynaptic membrane of the dendrite (*D*) may contain a trace of reaction product (large arrows), however. Dendritic mitochondria (*Md*) and ER membranes (*ERd*) as well as some Schwann cell (*Sc*) ER membranes (*ERs*) are lightly stained. To the left, a perikaryonal (*P*) plasma membrane (small arrow) and rough ER (*rER*) also show a trace of staining. × 50,500. Bar, 0.5 μm.

glial and Schwann cells, and of most of the similar enzyme of the rat, propionylcholinesterase (PrChE), to glial and other non-neuronal cells in the CNS (30), along with reports of high concentrations of BuChE and minimal amounts of AChE in various types of gliomas (7, 8, 70). The physiological function of BuChE is unknown, for its chronic selective inhibition produces no detectable consistent effects (25, 32, 63). The observations made here, of the identical localization of BuChE and AChE at postsynaptic sites in the cat SCG, suggested that BuChE, either synthesized locally or taken up from the plasma, might serve there as a precursor in the synthesis of AChE. Evidence consistent with this hypothesis has been obtained with the SCG and other autonomic ganglia of the cat, where the persistent selective inactivation of BuChE by iso-OMPA was found to delay the regeneration of AChE after its inactivation by sarin (39). In the SCG of the rat, where both AChE and PrChE are present in the somata of high proportions of the adrenergic ganglion cells (16, 30), this relationship does not appear to apply.[1]

The valuable technical assistance of Mrs. Ashley Fine Nagle and Mrs. Eloise Gabel Smyrl is acknowledged with thanks. We are indebted to the following donors for generous supplies of the compounds indicated: Dr. R. Dahlbohm, Astra Lakemedel AB, Stockholm, (Astra 1397); Dr. V. Sim, Biomedical Laboratories, Edgewood Arsenal, Md., (sarin); Dr. Daniel L. Shaw, Jr., Wyeth Laboratories, Radnor, Pa., (mephentermine); Burroughs Wellcome, Inc., Research Triangle Park, N.C., (B. W. 284). Fig. 20 was prepared by Mrs. Alma Hamell.

[1] G. B. Koelle, and E. G. Smyrl. Manuscript in preparation.

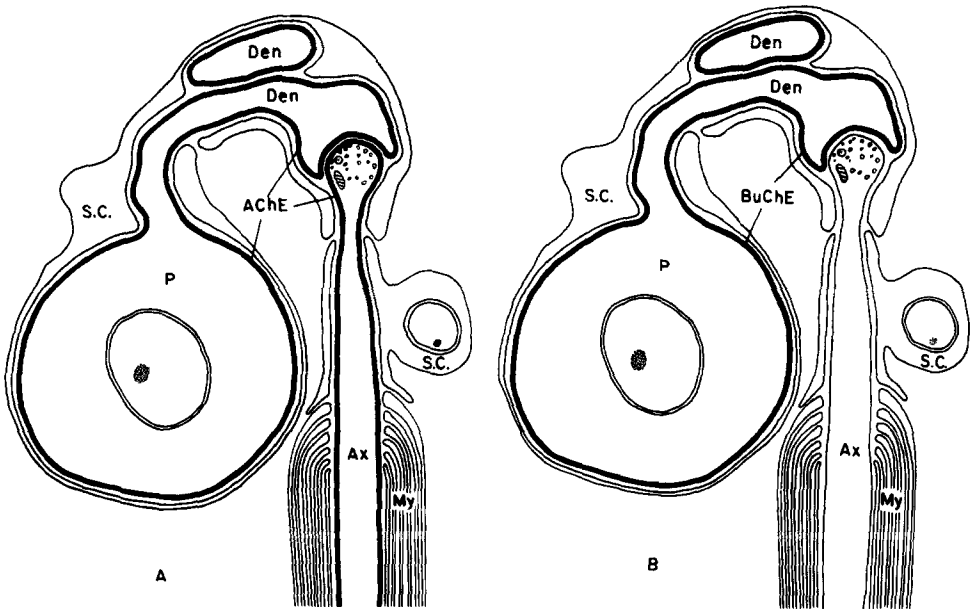

FIGURE 20 A diagrammatic representation of the localization of AChE and BuChE demonstrated in the present study. In Figure 20*A*, AChE is shown as the bold line representing the axolemma of the innervating cholinergic axon (*Ax*) where it is myelinated (*My*) and where it is unmyelinated, or covered only by a sheath of Schwann cell (*Sc*) cytoplasm, down to and including the axodendritic contact. The enzyme is also localized on the plasma membrane of the postsynaptic dendrites (*Den*) and the perikaryon (*P*). BuChE (Fig. 20*B*) is localized only in the plasmalemma of the postsynaptic ganglion cell (*P*) and its dendrites (*Den*). Not included in the diagram are the numerous other dendrites issuing from the perikaryon which also possess AChE and BuChE, and the intracellular organelles in which we can not determine definitely whether or not cholinesterase enzymes are present due to the interference of nonspecific esterases, i.e., persistence of significant staining in the presence of physostigmine. The postganglionic axon, which probably arises from a dendrite at some distance from the cell body, is not depicted; however, on the basis of numerous reports of LM and EM histochemistry, it is likely that it is devoid of significant concentrations of AChE or BuChE.

This investigation was supported by Research Grants NS-00282-19-25 from the National Institute of Neurological and Communicative Disorders and Stroke, National Institutes of Health, United States Public Health Service.

Received for publication 26 January 1978, and in revised form 28 April 1978.

REFERENCES

1. BARRNETT, R. J. 1962. The fine structural localization of acetylcholinesterase at the myoneural junction. *J. Cell Biol.* **12**:247–262.
2. BELL, M., and R. J. BARRNETT. 1965. The use of thiol-substituted carboxylic acids as histochemical substrates. *J. Histochem. Cytochem.* **13**:611–628.
3. BILLINGSLEY, P. R., and S. W. RANSON. 1918. Branches of the ganglion cervicale superius. *J. Comp. Neurol.* **29**:367–384.
4. BIRKS, R. I. 1974. The relationship of transmitter release and storage to fine structure in a sympathetic ganglion. *J. Neurocytol.* **3**:133–160.
5. BRIGHTMAN, M. W., and R. W. ALBERS. 1959. Species differences in the distribution of extraneuronal cholinesterases within the vertebrate central nervous system. *J. Neurochem.* **4**:244–250.
6. BRZIN, M., V. M. TENNYSON, and P. E. DUFFY. 1966. Acetylcholinesterase in frog sympathetic and dorsal root ganglia. *J. Cell Biol.* **31**:215–242.
7. BÜLBRING, E., F. J. PHILPOT, and F. D. BOSANQUET. 1953. Amine oxidase, pressor amines, and cholinesterase in brain tumours. *Lancet.* **1**:865–866.
8. CAVANAGH, J. B., R. H. S. THOMPSON, and G. R. WEBSTER. 1954. The localization of pseudocholinesterase activity in nervous tissue. *Q. J. Exptl. Physiol. Cogn. Med. Sci.* **39**:185–197.
9. CSILLIK, B. 1975. Synaptochemistry of acetylcholine metabolism in a cholinergic neuron. *Int. Rev. Neurobiol.* **18**:69–140.
10. DAVIS, R., and G. B. KOELLE. 1967. Electron

microscopic localization of acetylcholinesterase and nonspecific cholinesterase at the neuromuscular junction by the gold-thiocholine and gold-thiolacetic acid methods. *J. Cell Biol.* **34**:157–171.

11. De Castro, F. 1932. Sympathetic ganglia, normal and pathological. *In* Cytology and Cellular Pathology of the Nervous System. W. Penfield, editor. Hafner Publishing Co., New York. vol. 1. 319–379.
12. Droz, B. 1975. Synthetic machinery and axoplasmic transport: maintenance of neuronal connectivity. *In* The Nervous System. D. B. Tower, editor. Raven Press, New York. vol. 1. 111–127.
13. Droz, B., H. L. Koenig, and L. Di Giamberardino. 1973. Axonal migration of protein and glycoprotein to nerve endings. I. Radioautographic analysis of the renewal of protein in nerve endings of chicken ciliary ganglion after intracerebral injection of [^{3}H]lysine. *Brain Res.* **60**:93–127.
14. Elfvin, L.-G. 1963. The ultrastructure of the superior cervical sympathetic ganglion of the cat. I. The structure of the ganglion cell processes as studied by serial sections. *J. Ultrastruct. Res.* **8**:403–440.
15. Elfvin, L.-G. 1963. The ultrastructure of the superior cervical sympathetic ganglion of the cat. II. The structure of the preganglionic end fibers and the synapses as studied by serial sections. *J. Ultrastruct. Res.* **8**:441–476.
16. Eränkö, L. 1972. Biochemical and histochemical observations on the postnatal development of cholinesterases in the sympathetic ganglion of the rat. *Histochem. J.* **4**:545–559.
17. Eränkö, O., and M. Härkönen. 1965. Monoamine-containing small cells in the superior cervical ganglion of the rat and an organ composed of them. *Acta Physiol. Scand.* **63**:511–512.
18. Eränkö, O., G. B. Koelle, and L. Räisänen. 1967. A thiocholine-lead ferrocyanide method for acetylcholinesterase. *J. Histochem. Cytochem.* **15**:674–679.
19. Esterhuizen, A. C., J. D. P. Graham, J. D. Lever, and T. L. B. Spriggs. 1968. Catecholamine and acetylcholinesterase distribution in relation to noradrenaline release. An enzyme histochemical and autoradiographic study on the innervation of the cat nictitating muscle. *Br. J. Pharmacol. Chemother.* **32**:46–56.
20. Grillo, M. A. 1966. Electron microscopy of sympathetic tissue. *Pharmacol. Rev.* **18**:387–399.
21. Hámori, J., E. Láng, and L. Simon. 1968. Experimental degeneration of the preganglionic fibers in the superior cervical ganglion of the cat. *Z. Zellforsch. Microsc. Anat.* **90**:37–52.
22. Heuser, J. E., and T. S. Reese. 1973. Evidence for recycling of synaptic membrane during transmitter release at the frog neuromuscular junction. *J. Cell Biol.* **57**:315–344.
23. Holmstedt, B., and F. Sjöqvist. 1959. Distribution of acetocholinesterase in the ganglion cells of various sympathetic ganglia. *Acta Physiol. Scand.* **47**:284–296.
24. Jóo, F., D. Lever, C. Ivens, D. R. Mottram, and R. Presley. 1971. A fine structural and electron histochemical study of axon terminals in the rat superior cervical ganglion after acute and chronic preganglionic denervation. *J. Anat.* **110**:181–189.
25. Karczmar, A. G. 1967. Pharmacologic, toxicologic and therapeutic properties of anticholinesterase agents. *In* Physiological Pharmacology. Vol. III. W. S. Root, and F. G. Hofmann, editors. Academic Press, Inc., New York. 163–322
26. Kása, P. 1968. Acetylcholinesterase transport in the central and peripheral nervous tissue: the role of tubules in the enzyme transport. *Nature (Lond.).* **218**:1265–1267.
27. Kása, P., and E. Csernovszky. 1967. Electron microscopic localization of acetylcholinesterase in the superior cervical ganglion of the rat. *Acta Histochem.* **28**:274–285.
28. Kása, P., S. P. Mann, S. Karcsu, L. Tóth, and S. Jordon. 1973. Transport of choline acetyl transferase and acetylcholinesterase in the rat sciatic nerve: a biochemical and electron histochemical study. *J. Neurochem.* **21**:431–436.
29. Koelle, G. B. 1951. The elimination of enzymatic diffusion artifacts in the histochemical localization of cholinesterases and a survey of their cellular distributions. *J. Pharmacol. Exp. Ther.* **103**:153–171.
30. Koelle, G. B. 1954. The histochemical localization of cholinesterases in the central nervous system of the rat. *J. Comp. Neurol.* **100**:211–235.
31. Koelle, G. B. 1955. The histochemical identification of acetylcholinesterase in cholinergic, adrenergic and sensory neurons. *J. Pharmacol. Exp. Ther.* **114**:167–184.
32. Koelle, G. B. 1963. Cytological distributions and physiological functions of cholinesterases. *In* Cholinesterases and Anticholinesterase Agents. G. B. Koelle, editor. Springer-Verlag KG., Berlin. 187–298.
33. Koelle, G. B., R. Davis, and M. Devlin. 1968. Acetyl Disulfide, $(CH_3COS)_2$, and bis-(thioacetoxy) aurate (I) Complex, $Au(CH_3COS)_2$, histochemical substrates of unusual properties with acetylcholinesterase. *J. Histochem. Cytochem.* **16**:754–764.
34. Koelle, G. B., R. Davis, E. J. Diliberto, Jr., and W. A. Koelle. 1973. Selective, near-total, irreversible inactivation of peripheral pseudocholinesterase and acetylcholinesterase in cats *in vivo*. *Biochem. Pharmacol.* **23**:175–188.
35. Koelle, G. B., R. Davis, and W. A. Koelle. 1974. Effects of aldehyde fixation and of preganglionic denervation on acetylcholinesterase and butyrocholinesterase of cat autonomic ganglia. *J. His-*

tochem. Cytochem. **22**:244–251.

36. KOELLE, G. B., R. DAVIS, E. G. SMYRL, and A. V. FINE. 1974. Refinement of the bis-(thioacetoxy) aurate (I) method for the electron microscopic localization of acetylcholinesterase and nonspecific cholinesterase. *J. Histochem. Cytochem.* **22**:252–259.
37. KOELLE, G. B., and C. FOROGLOU-KERAMEOS. 1965. Electron microscopic localization of cholinesterases in a sympathetic ganglion by a gold-thiolacetic acid method. *Life Sci.* **4**:417–424.
38. KOELLE, G. B., and C. G. GROMADZKI. 1966. Comparison of the gold-thiocholine and gold-thiolacetic acid methods for the histochemical localization of acetylcholinesterase and cholinesterases. *J. Histochem. Cytochem.* **14**:443–454.
39. KOELLE, G. B., W. A. KOELLE, and E. G. SMYRL. 1977. Effects of inactivation of butyrylcholinesterase on steady state and regenerating levels of ganglionic acetylcholinesterase. *J. Neurochem.* **28**:313–319.
40. KOELLE, G. B., and E. C. STEINER. 1956. The cerebral distributions of a tertiary and a quaternary anticholinesterase agent following intravenous and intraventricular injection. *J. Pharmacol. Exp. Ther.* **118**:420–434.
41. KOELLE, W. A., K. S. HOSSAINI, P. AKBARZADEH, and G. B. KOELLE. 1970. Histochemical evidence and consequences of the occurrence of isoenzymes of acetylcholinesterase. *J. Histochem. Cytochem.* **18**:812–819.
42. KOELLE, W. A., and G. B. KOELLE. 1959. The localization of external or functional acetylcholinesterase at the synapses of autonomic ganglia. *J. Pharmacol. Exp. Ther.* **126**:1–8.
43. KOELLE, W. A., E. G. SMYRL, G. A. RUCH, V. E. SIDDONS, and G. B. KOELLE. 1977. Effects of protection of butyrylcholinesterase on regeneration of ganglionic acetylcholinesterase. *J. Neurochem.* **28**:307–311.
44. KOENIG, E., and G. B. KOELLE. 1961. Mode of regeneration of acetylcholinesterase in cholinergic neurons following irreversible inactivation. *J. Neurochem.* **8**:169–188.
45. LAKOS, I. 1970. Ultrastructure of chronically denervated superior cervical ganglion in the cat and rat. *Acta Biol. Acad. Sci. Hung.* **21**:425–427.
46. LEWIS, P. R., and D. P. KNIGHT. 1977. Staining methods for sectioned material. North-Holland Publishing Company, Amsterdam. 311 pp.
47. LEWIS, P. R., and C. C. D. SHUTE. 1969. An electron microscopic study of cholinesterase distribution in the rat adrenal medulla. *J. Microsc. (Oxf.).* **89**:181–193.
48. LUBIŃSKA, L. 1964. Axoplasmic streaming in regenerating and in normal nerve fibers. *In* Mechanisms of Neural Regeneration. M. Singer, and J. P. Schade, editors. Progress in Brain Research, vol. 13. Elsevier Scientific Publishing Company, Amsterdam.
49. LUBIŃSKA, L., and S. NIEMIERKO. 1971. Velocity and intensity of bidirectional migration of acetylcholinesterase in transected nerves. *Brain Res.* **27**:329–342.
50. LUFT, J. H. 1961. Improvements in epoxy resin embedding methods. *J. Biophys. Biochem. Cytol.* **9**:409–414.
51. MATSUURA, H., M. MORI, and K. KAWAKATSU. 1969. A histochemical and electronmicroscopic study of the trigeminal ganglion of the rat. *Arch. Oral Biol.* **14**:1135–1146.
52. MATTHEWS, M. R. 1974. Ultrastructure of ganglionic junctions. *In* The Peripheral Nervous System. J. I. Hubbard, editor. Plenum Press, New York. 111–150.
53. NACHMANSOHN, D., and E. NEUMANN. 1975. Chemical and Molecular Basis of Nerve Activity. Academic Press, Inc., New York. 403 pp.
54. OCHS, S. 1974. Axoplasmic transport-energy metabolism and mechanism. *In* The Peripheral Nervous System. J. I. Hubbard, editor. Plenum Press, New York. 47–72.
55. OCHS, S. 1975. Mechanism of axoplasmic transport and its block by pharmacological agents. L. Ahtee, editor. Proceedings of the Sixth International Pharmacological Congress. Helsinki, Finland. **2**: 161–174.
56. PALADE, G. E.. 1952. A study of fixation for electron microscopy. *J. Exp. Med.* **95**:285–298.
57. PÁRDUCZ, Á., O. FEHÉR, and F. Jóo. 1971. Effects of stimulation and hemicholinium (HC-3) on the fine structure of nerve endings in the superior cervical ganglion of the cat. *Brain Res.* **34**:61–72.
58. PYSH, J. J., and R. G. WILEY. 1974. Synaptic vesicle depletion and recovery in cat superior cervical ganglion electrically stimulated *in vivo*. *J. Cell Biol.* **60**:365–374.
59. RANISH, N., and S. OCHS. 1972. Fast axoplasmic transport of acetylcholinesterase in mammalian nerve fibers. *J. Neurochem.* **19**:2641–2649.
60. RANSON, S. W., and P. R. BILLINGSLEY. 1918. The superior cervical ganglion and the cervical portion of the sympathetic trunk. *J. Comp. Neurol.* **29**:313–358.
61. ROESSMANN, U., and R. L. FRIEDE. 1966. Changes in butyrylcholinesterase activity in reactive glia. *Neurology.* **16**:123–129.
62. SAWYER, C. H., and W. H. HOLLINSHEAD. 1945. Cholinesterases in sympathetic fibers and ganglia. *J. Neurophys.* **8**:135–153.
63. SILVER, A. 1974. The biology of cholinesterases. American Elsevier Publishing Co. Inc., New York. 447 pp.
64. TUCEK, S. 1975. Transport of choline acetyltransferase and acetylcholinesterase in the central stump and isolated segments of a peripheral nerve. *Brain*

Res. **86**:259–270.

65. WASCHSTEIN, M., E. MEISEL, and C. FALCON. 1961. Histochemistry of thiolacetic acid esterase: a comparison with nonspecific esterase with special regard to the effect of fixatives and inhibitors on intracellular localization. *J. Histochem. Cytochem.* **9**:326–339.
66. WEISS, P., and H. B. HISCOE. 1948. Experiments on the mechanism of nerve growth. *J. Exp. Zool.* **107**:315–395.
67. WEITSEN, H. and F. F. WEIGHT. 1977. Synaptic innervation of sympathetic ganglion cells in the bullfrog. *Brain Res.* **128**:197–211.
68. WESTRUM, L. E., and S. H. BRODERSON. 1976. Acetylcholinesterase activity of synaptic structures in the spinal trigeminal nucleus. *J. Neurocytol.* **5**:551–563.
69. WILLIAMS, T. H., T. CHIBA, A. C. BLACK, JR., R. C. BHALLA, and J. JEW. 1976. Species variation in SIF cells of superior cervical ganglia: are there two functional types? *In* SIF Cells, Structure and Function of the Small, Intensely Fluorescent Sympathetic Cells. O. Eränkö, editor. DHEW Publication No. (NIH) 76-942. Washington, D.C. 143–162.
70. WOLLEMANN, M., and L. ZOLTAN. 1962. Cholinesterase activity of cerebral tumors and tumorous cysts. *Arch. Neurol. Psychiatry.* **6**:161–167.